TRANSFECTION EFFICIENCIES OF CHITOSAN/SIRNA NANOPARTICLES IN COLORECTAL CANCER CELLS

THESIS

Presented to the Graduate Council of
Texas State University-San Marcos
In Partial Fulfillment
of the Requirements

for the Degree

Master of SCIENCE

by

Adriana S. Palacios, B.A.

San Marcos, Texas
December 2012

TRANSFECTION EFFICIENCIES OF CHITOSAN/SIRNA NANOPARTICLES IN COLORECTAL CANCER CELLS

Committee Members Approved:

Walter E. Rudzinski, Chair

Steven T. Whitten

Tania Betancourt

Approved:

J. Michael Willoughby
Dean of the Graduate College

FAIR USE AND AUTHOR'S PERMISSION STATEMENT

FAIR USE

Duplication Permission

DEDICATION

To Eduardo Soliz Jr.
my grandfather
who always encouraged me to “stick to the books.”

ACKNOWLEDGEMENTS

First I would like to acknowledge my committee members: Dr. Walter E. Rudzinski, Dr. Steven T. Whitten, and Tania Betancourt who have spent countless hours with me mentoring and tutoring me. Secondly, I would like to acknowledge Dr. Michelle A. Lane who has mentored me as a woman in science (professionally and personally) and who I could not have gotten through this program without. Thirdly, I would like to acknowledge those professors whose equipment I have used throughout this project and whose knowledge has helped me tremendously: Dr. Joseph R. Koke, Dr. Ron Walter, and Dr. Dana Garcia. I would also like to acknowledge Mrs. Alissa Savage and Mr. Eric Shires for the hours they spent working on training me and helping me work the instruments. Also to Ms. Sarah Kane, and Ms. Kaylan Olds who have answered many of my questions. I would also like to acknowledge the rest of my colleagues in the Biochemistry Department and to the rest of my lab group: Mr. Abuzar Ahmed, Mr. Edgar Vargas, and Mr. Shachindra Nargund who I could not have gotten through this process without. Lastly, the person that I would especially like to thank the most is my husband, Aaron R. Palacios for being my biggest cheerleader and supporter during this long and arduous process.

This manuscript was submitted on July 2012 for final review.

TABLE OF CONTENTS

Page

ACKNOWLEDGEMENTS vi

LIST OF TABLES ix

LIST OF FIGURES x

ABSTRACT xii

CHAPTER

I. INTRODUCTION 1

1.1 RNAi 1
1.2 Delivery Vehicles 3
Bacterial and Viral Vehicles 3
Non-Viral Vehicles 3
1.3 Chitosan 4
Chitosan Properties 4
Chitosan Nanoparticles 5
Chitosan with Polyethylene Glycol (Chitosan-PEG) Nanoparticles 6
1.4 Research Strategy 7

II. MATERIALS AND METHODS 9

2.1 Materials 9
2.2 Preparation of Chitosan and Chitosan/siRNA Nanoparticles 10
2.3 Evaluation of siRNA Loading Efficiency 11
2.4 Characterization of Chitosan and Chitosan/siRNA Nanoparticles 12
2.5 Culture of HCT 116 Human Carcinoma Cells 13
2.6 Evaluation of Transfection of siRNA Nanoparticles Using Laser Scanning Confocal Microscopy 14
2.7 Evaluation of Transfection of Chitosan/siRNA Nanoparticles Using Live Cell Imaging 16

III. RESULTS 17

3.1 Evaluation of siRNA Loading Efficiency 17

3.2 TEM Characterization of Nanoparticles 18
3.3 SEM and EDS Characterization of Nanoparticles 19
3.4 Dynamic Light Scattering Analysis of Nanoparticles 23
3.5 Confocal Microscopy Characterization of Nanoparticles 24
3.6 Evaluation of Transfection of siRNA Nanoparticles Using Laser Scanning Confocal Microscopy 25
Control 26
12 Hours Post Transfection 27
24 Hours Post Transfection 30
48 Hours Post Transfection 32
3.7 Evaluation of Transfection of Chitosan/siRNA Nanoparticles Using Live Cell Imaging 34

IV. DISCUSSION 38

4.1 Size 38
4.2 Incorporation of siRNA 42
4.3 Transfection of siRNA Via Chitosan Based Nanoparticles 43
Classic Confocal Evaluation: 12, 24, and 48 Hours Post Transfection 43
Live Cell Imaging Evaluation 44

APPENDIX A: SUPPLEMENTAL MATERIALS 46

REFERENCES 47

LIST OF TABLES

Table **Page**

1. ImageJ Size Analysis 20
2. EDS Quantification of Chitosan Nanoparticles 23
3. EDS Quantification of Chitosan/siRNA Nanoparticles 23
4. DLS Size Analysis 23

LIST OF FIGURES

Figure **Page**

1. Deacetylation of Chitin 4
2. Absorbance as a Function of siRNA Concentration 17
3. TEM Image of Chitosan Nanoparticles 18
4. TEM Image of Chitosan/siRNA Nanoparticles 19
5. SEM Image of Chitosan/siRNA Nanoparticles at Low Magnification 19
6. SEM Characterization of Nanoparticles 20
7. SEM Average Size of Nanoparticles 21
8. EDS of Nanoparticles 22
9. DLS Average Size of Nanoparticles 24
10. Confocal Characterization of Nanoparticles 25
11. Control Cells 26
12. Histogram of Control Cells 27
13. 12 Hours Post Transfection 28
14. Histogram of 12 Hours Cells 29
15. 12 Hour Cells Turned on X Axis 30
16. 24 Hours Post Transfection 31
17. Histogram of 24 Hour Cells 32
18. 48 Hours Post Transfection 33
19. Histogram of 48 Hour Cells 34

20. Lipofectamine 2000/ siRNA Live Cell Images 35

21. Chitosan/siRNA Live Cell Images.....36

ABSTRACT

TRANSFECTION EFFICIENCIES OF CHITOSAN/SIRNA NANOPARTICLES IN COLORECTAL CANCER CELLS

by

Adriana Soliz Palacios, B.A.

Texas State University-San Marcos

December 2012

SUPERVISING PROFESSOR: WALTER E. RUDZINSKI

RNA interference (RNAi) is a recently discovered phenomenon that employs the use of miRNA (microRNA) and siRNA (short interfering RNA) that can be utilized for gene therapy purposes. However, the problem that has arisen is delivery of the siRNAs into diseased cells. The compound chitosan has recently gained much attention because it possesses several properties that make it an ideal candidate as a delivery vehicle for siRNA. Chitosan/siRNA based nanoparticles have been synthesized and characterized that are less than 100 nm in diameter. Characterization of their size was completed by using transmission electron microscopy (TEM), scanning electron microscopy (SEM), and dynamic light scattering (DLS) techniques. Characterization of siRNA loading was

accomplished by utilizing UV spectroscopy, EDS, and confocal microscopy to test encapsulation of siRNA. The colorectal cancer cell line HCT 116, was used to test transfection of siRNA across the cellular membrane. The transfection efficiencies were evaluated by using fluorescently tagged siRNA embedded within chitosan nanoparticles. The chitosan/siRNA delivery system was compared with the classical approach used for siRNA delivery; namely, siRNA in Lipofectamine 2000 as well as with cells that received no treatment. Live cell imaging was also employed to aid in visualization of transfection. The results show that the chitosan based systems do transfect siRNA across the cellular member.

CHAPTER I

INTRODUCTION

Since the discovery of RNA interference (RNAi) in 1998,[1] this technology has emerged as a potential new therapeutic strategy to help solve some of the most debilitating human diseases. From HIV to a variety of cancers, RNAi and its mechanisms have shown that gene silencing is a natural pathway that can be utilized to mitigate some of the effects of disease.[2-6] We now possess the understanding and technology that is needed to harness this pathway for gene therapy applications.

1.1 RNAi

The basis of RNA interference is sequence specific degradation of mRNA for eventual protein knockdown. There has been speculation as to why this pathway has developed and evolved primarily in eukaryotes, and the evidence at this point in time suggests that RNAi is a defense against foreign RNA (introduced by viruses or transposons) and also it is another mechanism for gene regulation/expression.[6] There are two pathways within RNAi: one that involves small inhibiting RNA, also called siRNA, and one that involves micro RNA or miRNA. What we are particularly interested in is the siRNA pathway. The siRNA pathway first starts with a long piece of double stranded RNA in the cytoplasm of the cell. This long piece of dsRNA can originate from endogenous genes and introns or it can be exogenously introduced. Next, a cytoplasmic endoribonuclease called Dicer, comes in and cleaves the dsRNA to about 20 to 25

nucleotides long. A complex called RNA-induced silencing complex or RISC then selects one of the strands known as the guide strand and degrades the other strand known as the passenger strand. The guide strand guides RISC to the mRNA that is its complement. Not much is known about how complimentary the two strands have to be for the RISC complex to recognize the mRNA, but what is known is the recognition is usually near the 5' end or the least thermodynamically stable end of the guide strand.[2] Current research is investigating the exact amount of bases that are necessary for recognition. The RISC complex has a catalytic protein called Argonaut 2 which has a catalytic domain called the piwi domain which then proceeds to cleave the mRNA to a point to where it can no longer be functional. This action causes the gene knockdown or silencing.

Compared to other antisense pathways, RNAi is much more effective at silencing making it an ideal candidate to utilize.[2, 6] Exogenously introduced siRNA has several potential uses. Several human diseases have been associated with an expression of an altered protein or an over expression of a particular protein.[2, 4-6] The thought is that the RNAi pathway can be used to suppress these altered proteins or proteins that are overexpressed, and the diseased state of the cell can effectively be silenced. Some of the advantages of using RNAi are that the genome is not altered, and that the cell can still perform normal functions.[2, 6] However, previous research has found that nucleic acids such as siRNA are difficult to employ in practice because of degradation from nucleases, difficulty circulating in the bloodstream due to their inherent instability, a lack of specificity toward target cells, and an inability to penetrate the lipid bilayer.[4, 5, 7, 8] An ideal delivery vehicle must be developed to overcome these cellular obstacles, deliver the

gene therapy to specific targets, release the therapy precisely when needed all without having any toxic effect on the organism.

1.2 Delivery Vehicles

Over the past couple of years there have been several different proposals of what to use as a delivery vehicle for siRNA and three main classes have emerged: bacterial vehicles, viral vehicles, and non-viral vehicles.

Bacterial and Viral Vehicles

Most viral and bacterial vehicles induce a host immunosuppressant response when studied in vivo[4, 9] although this is not true for every viral or bacterial vehicle.[2] One other detriment of using these organisms is that they can rapidly evolve to either incorporate this technology for their own use or to become resistant to it.[6] Thus their application in therapy would be very limited and it adds another requirement that a delivery vehicle must overcome. However there are applications where it may be useful to utilize this technology such as treatment to combat other viruses or bacteria.[2]

Non-Viral Vehicles

Non-viral vehicles on the other hand show a greater promise than viral vehicles and are further divided into four classes: lipids, polymers, dendrimers, and polypeptides.[7] Polypeptides have not shown high transfection efficiencies and exhibit low endosomal escape.[7] The current research suggests that the mechanism for cellular uptake is not well known for polypeptides.[7] Dendrimers on the other hand show high transfection efficiencies but it has only been for certain types of cells. In addition to that there are cytotoxic effects and they have a low bioavailability.[7] Polymers present a different set of problems. They too tend to have cytotoxic effects along with low transfection

efficiencies; however, they can undergo modifications easily to fix these problems.[4] Lipids have high transfection efficiencies and are now the gold standard when conducting in vitro studies but they also have high cytotoxic effects on cells.[7] Although each class presents its own advantages and disadvantages one compound that has recently attracted a great deal of attention is chitosan found in the polymer class.

1.3 Chitosan

Chitosan Properties

Chitosan is a linear polysaccharide composed of repeating glycosidically linked β-(1-4)-D-glucosamine and N-acetyl-D-glucosamine. Chitosan is relatively inexpensive and

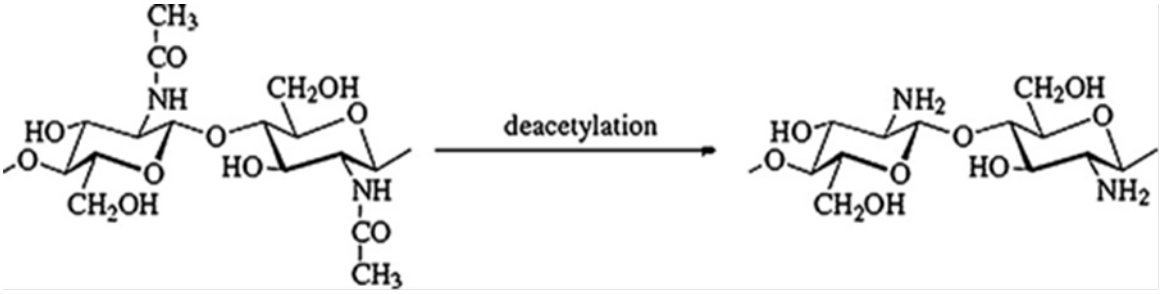

Figure 1. Deacetylation of Chitin.[19] Chitin deacetylated to form chitosan.

it is produced commercially by deacetylating chitin[10-17] as shown in Figure 1. Chitin is found naturally in the exoskeletons of most crustaceans as well as the cell walls of fungi. Chitosan is also widely available due to the fact that chitin is the second most abundant sugar in the world.[13] Because chitosan is a sugar, it is relatively non-toxic and has an LD50 of 16g/kg in rats.[9] In fact chitosan is currently being investigated for tissue engineering applications because it can promote cell growth and reduce local inflammation.[13] This bioavailability and non-toxic effects are what have made it so popular. What especially makes it an ideal gene delivery vehicle is the cationic property

of the amine group. The primary amine group in every deacetylated subunit has a pKa value of about 6.5 which makes it ideal to electrostatically bind to the negatively charged phosphate group in the siRNA. Studies have shown that this interaction leads to stability of the nanoparticle in the bloodstream, facilitates cellular uptake, and endosomal escape.[18] The amine groups also provide a site for a side group attachment to increase biofunctionality of the particle.

Chitosan Nanoparticles

Currently there are several different formulations for preparing chitosan/siRNA nanoparticles and they include: coacervation, ionic gelation, emulsion, covalent cross-linking, and desolvation. All of these formulation approaches influence the properties of the nanoparticles that affect transfection efficiencies. However there is no consensus on the best approach and further investigations need to be done to determine the optimum preparation protocol and formulation for gene delivery.[10, 13]

There are several properties of the chitosan/siRNA nanoparticles that influence the efficiency of transfection. One property is the molecular weight (Mw) of the chitosan. The Mw of chitosan influences the particle's size, stability, and ability to escape the endosome. The weight needs to be high enough to withstand the harsh extracellular environment, but it also must be low enough to be able to release the siRNA once it is within the cytoplasm. Studies have shown that a Mw between 114 and 170 kDa results in the highest transfection efficiencies.[9, 19] However, this is an approximation and not a definitive answer as to what the Mw should be. Another important property along with Mw is the nanoparticle size. The size of the particle must be large enough to encapsulate

the siRNA and protect it from the extracellular environment, but small enough to facilitate the release of the siRNA and penetrate the cell wall.[9, 19]

The degree of deacetylation (DD) of the chitosan also influences chitosan's biofunctionality. As mentioned above, the DD contributes to the particles stability and its ability to escape the endosome along with its solubility in solution. One drawback of using chitosan relates to its aggregation in solution which is related to its DD.[19] There has been much research in this area and it is a consensus that the DD of the Chitosan/siRNA should be around 80% to give the optimum transfection.[9]

One last property of the complexed nanoparticle that affects transfection is the nitrogen to phosphate ratio (N/P). This is the ratio between the chitosan nitrogen and the phosphate in the nucleotide backbone which gives the particle its overall surface charge and aids in endosomal escape as well. The ratio also affects the condensation of the siRNA for better stability and entrapment and improves the interaction with the negatively charged cell membrane. Recent studies have indicated that an N/P ratio of 150 results in the highest transfection efficiencies but only when compared to ratios of 50.[20]

Chitosan with Polyethylene Glycol (Chitosan-PEG) Nanoparticles

Although chitosan has many advantages, there are also several disadvantages. Chitosan is not very soluble at the pH of the bloodstream and it is also susceptible to degradation. One way to circumvent the disadvantage is to chemically modify some of the amine sites on the chitosan with polyethylene glycol (PEG). PEG can impart more hydrophilicity to the chitosan and also protect the nanoparticle from degradation. In one experiment, chitosan grafted with PEG showed a higher transfection efficiency of DNA and prevented aggregation when tested in the presence of serum and bile.[21]

1.4 Research Strategy

The transfection efficiency of chitosan and chitosan-PEG nanoparticles will be assessed using siRNA tagged with the red fluorophore AlexaFluor 555 and confocal microscopy. Transfection efficiency specifically means in this case entrance into the cell. The nanoparticles will first be prepared in a small, narrow size range. The loading efficiency of siRNA onto both types of particles will be assessed indirectly using UV spectroscopy by determining the amount of free siRNA after mixing with chitosan. The absorption or encapsulation of the siRNA into the chitosan nanoparticles will also be characterized using energy-dispersive x-ray spectroscopy and confocal imaging. The size and morphology of the chitosan and chitosan/siRNA particles will be assessed using three different techniques: transmission electron microscopy (TEM), scanning electron microscopy (SEM), and dynamic light scattering (DLS) analysis. To determine transfection efficiency in colorectal cancer cell lines, HCT 116 (provided by Dr. Michelle Lane) will be transfected with chitosan/siRNA and chitosan-PEG/siRNA nanoparticles, then imaged via confocal microscopy. The transfection efficiency of the nanoparticles will be compared with that of Lipofectamine 2000 (positive control) and cells without treatment (negative control). Finally, live cell imaging will be used to monitor the transfection of the fluorescently tagged siRNA in chitosan/siRNA nanoparticles over time.

Some of the questions that this thesis hopes to answer are: Can chitosan/siRNA nanoparticles below 100 nm be prepared? Do these nanoparticles actually incorporate the fluorescently labeled siRNA? If both of these questions can be answered, the next

question to ask is can these nanoparticles transfect fluorescently labeled siRNA into colorectal cancerous cells and if so how efficiently?

CHAPTER II

MATERIALS AND METHODS

2.1. Materials

Low molecular weight chitosan and sodium triphosphate pentabasic (TPP) were purchased from Sigma-Aldrich (St. Louis, MO, USA). Glacial acetic acid, HPLC grade methanol, and RNase free water were obtained from Fisher Scientific (Fair Lawn, NJ, USA). Sodium hydroxide was purchased from EM Science (Gibbstown, NJ, USA). 0.45µm 25mm nylon syringe filters (Pall Life Sciences), 0.22µm 25 mm nylon syringe filters, Hoechst 33342 nuclear stain, 90% glycerol, 97% paraformaldehyde (Alfa Aesar), 18mm round glass slipcovers, and frosted glass slides were purchased from VWR International (Radnor, PA, USA). A twenty one base pair siRNA with an AlexaFluor 555 fluorescent tag on the 5' end and a sense strand of 5'- UCUCCGAACGUGUCACGUTT -3' and an antisense strand of 5'- ACGUGACACGUUCGGAGAATT -3' scrambled siRNA was purchased from Qiagen (Germantown, MD, USA). Lipofectamine 2000 was purchased from Life Technologies (Grand Island, NY, USA).

Aluminum tape, formvar coated nickel transmission electron microscope grids, and 2% phosphotungstic acid were generously donated by Dr. Joseph R. Koke (Texas State University-San Marcos, Department of Biology). Dulbecco's modified eagle medium (DMEM), fetal bovine serum (FBS), 10x trypsin, phosphate buffered saline

(PBS), and Pen/Strep (1000 U/ml of penicillin and 1000 µg/ml of streptomycin), and HCT-116 cell line were generously donated by Dr. Michelle Lane (Texas State University-San Marcos, Department of Family and Consumer Sciences).Chemically modified chitosan with poly ethylene glycol (chitosan-PEG)/siRNA nanoparticles were prepared by Mr. Abuzar Ahmed.

2.2 Preparation of Chitosan and Chitosan/siRNA Nanoparticles

Chitosan and chitosan/siRNA nanoparticles were prepared using an ionic gelation method that has been described previously.[22] Briefly 25 mg of low molecular weight chitosan was dissolved in 5 mL of 0.85% acetic acid, and then stirred for 10 minutes. The solution was sonicated for 5 minutes, and finally stirred again for 5 minutes. The pH of the solution was then adjusted to 4.6 using 1 M sodium hydroxide (NaOH). The chitosan solution was then filtered through a 0.45 µm and then 0.22 µm nylon syringe filters. In a separate beaker, 140 µl of 0.25% TPP and 35 µg of siRNA were mixed together. The chitosan/ siRNA nanoparticles were formed spontaneously when the TPP/siRNA solution was added very slowly to 525 µl of chitosan solution. Specifically about 25 µl of TPP/siRNA solution was added to the chitosan solution and then vortexed for 5 seconds. This was repeated until all of the TPP/siRNA solution was added to the chitosan solution. Chitosan nanoparticles were formed using the same manner as described above except siRNA was not contained in the TPP solution.

The nanoparticle solutions were then refrigerated at 4°C for one hour to stabilize the nanoparticles. The nanoparticles were concentrated by centrifugation at 13467 x g (G-force), for 120 minutes at 4°C using an Allegra 25R centrifuge from Beckman Coulter (Fullerton, CA, USA). The pelleted nanoparticles were placed in 525 µl of RNase free

water and vortexed vigorously until evenly suspended. The supernatants were saved for evaluation of siRNA loading efficiency.

2.3 Evaluation of siRNA Loading Efficiency

A ladder containing serial dilutions of siRNA at different known concentrations was prepared and tested for absorbance at a wavelength of 260 nm using the NanoDrop system (Thermo Scientific, Wilmington, DE, USA). The NanoDrop system is capable of measuring the absorbance of as little as 1µl. Absorbance was plotted against the concentration of siRNA to obtain a standard curve. Three points closest to the unknown absorbance of unassociated siRNA were then used in the calculation of the slope of the standard curve. Next, the absorbance of the supernatant from chitosan (non-encapsulated) nanoparticles was taken and used as a blank. Then, the supernatant was measured to ensure that the blank was calibrated properly. The absorbance of supernatant from chitosan/siRNA nanoparticles was then measured three times in the same manner as the chitosan nanoparticles and then averaged.

The amount of siRNA in the supernatant was then calculated using the equation from the slope of the standard curve. The amount of free siRNA in the supernatant was then subtracted from the total amount of siRNA added to the chitosan solution, divided by the total amount of siRNA, and multiplied by 100 to give a percentage. This percentage was used to evaluate the loading efficiency of siRNA into the chitosan nanoparticles. This same procedure was used to evaluate the loading efficiency of the chitosan-PEG/siRNA nanoparticles as well.

2.4 Characterization of Chitosan and Chitosan/siRNA Nanoparticles

The size and morphology of the chitosan, and chitosan/siRNA nanoparticles were determined using a transmission electron microscope (TEM) JEM 1200 EXII from JOEL Ltd. (Tokyo, Japan) and a scanning electron microscope (SEM) Helios NanoLab 400 DualBeam Scanning Electron Microscope from FEI Co. (Hillsboro, OR, USA). The size of the nanoparticles was also measured by dynamic light scattering (DLS) analysis by a Malvern Instruments Zetasizer Nano ZS (Herrenberg, Germany). Energy dispersive X-ray spectroscopy (EDS) data was acquired with the Apollo X silicon drift detector (SDD) with TEAM EDS system from EDAX (Mahwah, NJ, USA). Nanoparticle fluorescence was monitored by an Olympus FV1000 Laser Scanning Confocal Microscope with a 60x Olympus objective lens (NA: 1.40) (Tokyo, Japan). ImageJ, Adobe Photoshop, Olympus Fluoview 3.0 software, and Excel were employed for imaging and statistical analysis.

For TEM analysis, 1 µl of chitosan and chitosan/siRNA nanoparticles was added to 100 µl of RNase free water. Each TEM sample was then platted onto a nickel TEM grid and then stained with 2% phosphotungstic acid for 2.20 minutes. The grids were then taken off of the stain and allowed to air dry. Size and morphology were then observed with the TEM under vacuum conditions.

For SEM analysis, 1 µl of each sample was placed on a small piece of aluminum tape and allowed to air dry overnight. The size and morphology of the particles was observed, measured, and imaged in secondary and backscatter electron mode under vacuum. Next the TEAM EDS system imaged the area and did an elemental analysis for both types of nanoparticles.

The size of the nanoparticles was also obtained using dynamic light scattering by the Zetasizer Nano ZS.1µl of nanoparticles was placed into 1ml of RNase free water and then sonicated for 5 minutes. Size measurements were taken at 173° angle backscatter mode at 25°C.

To compare the fluorescence emanating from the AlexaFluor 555 tag conjugated to the siRNA in the chitosan/siRNA nanoparticles with a chitosan control, both of the TEM grids were placed on a glass slide in 90% glycerol under the laser scanning confocal microscope. The two samples were imaged under 60x oil immersion magnification (NA: 1.40) with 18 slices at 0.30 µm thick with the laser settings (405 nm: 8%; 559 nm: 10%) the same for both and the full z projection shown in every image.

2.5 Culture of HCT 116 Human Carcinoma Cells

To investigate whether or not these nanoparticle can actually penetrate a eukaryotic cell membrane, the human colon cancer cell line HCT-116 was cultured and used in these experiments as recommended by the American Type Culture Collection (Manassas, VA).

Cells were thawed and grown in 175 cm^2 culture flasks with DMEM media supplemented with 10% FBS and antibiotics (1000 U/ml of penicillin and 1000 µg/ml of streptomycin) for one week prior to use. Once the cells reached 80% confluence, they were detached by using 1x trypsin and counted using a Z1 Coulter particle counter (Beckman Coulter, Indianapolis, IN, USA). Since the cell line is adherent, non-coated round glass slipcovers were sterilized in 70% ethanol and then placed at the bottom of the wells before the cells and media were added. Cells were then plated in a 12-well plate at a density of 1.0 X 10^5 cells/well and incubated overnight in 10% FBS and antibiotic

supplemented DMEM. The cells were allowed to grow on the glass coverslips for 24 hours before either evaluation of transfection efficiency or for live cell imaging.

2.6 Evaluation of Transfection of siRNA Nanoparticles Using Laser Scanning Confocal Microscopy

Chitosan/siRNA and chitosan-PEG/siRNA nanoparticles were concentrated by centrifuging at 7889 x g for 10 minutes at room temperature with a Mini Spin Plus (Eppendorf AG, Hamburg, Germany). The resulting pellet was taken out and resuspended in 525 µl of DMEM culture media via mechanical separation and vortexing of the sample. The suspensions were then sterilized by passing the solutions through a 0.2 µm Millipore syringe filter (Billerica, MA, USA). The concentration of the nanoparticle solution was then adjusted to 100 nmol of siRNA per ml of DMEM by adding the appropriate amount of DMEM as determined by the loading efficiency results for both types of nanoparticles. Lipofectamine 2000 loaded with siRNA was used as a control and was prepared at a concentration of 200 pmol/µl according to the manufacturer's protocol. The media that was incubating the cells was removed and replaced by 500 µl of chitosan transfection media (either the chitosan/siRNA or chitosan-PEG/siRNA nanoparticles), or 253 µl of Lipofectamine 2000/siRNA transfecting media. These transfection media were allowed to incubate in the wells for 4 hours after which they were replaced with 1 ml of DMEM (non-supplemented).

Transfection into the HCT116 cells using the three different transfection media (Lipofectamine 2000/siRNA, chitosan/siRNA, or chitosan-PEG/siRNA nanoparticles) were evaluated via confocal microscopy at 12, 24, and 48 hours post transfection along with control cells that were not exposed to the transfection media. At the appropriate time, the DMEM culture media was taken out of the well and the cells that were

contained in the well were washed twice in sterile PBS for 10 minutes. A 4% solution of paraformaldehyde prepared from 37% paraformaldehyde and PBS and 1 ml of the 4% paraformaldehyde was added to the cells and allowed to sit for 10 minutes for fixation purposes. The paraformaldehyde was subsequently removed and three 10 minute washes with sterile PBS were performed. Then 1 ml of -80°C methanol was placed in the well and allowed to incubate in the wells for 5 minutes. It was subsequently removed and the cells were allowed to air dry for approximately 5 minutes. The cells were then washed again with sterile PBS for 10 minutes three times. In an effort to distinguish individual cells and to help distinguish where the nanoparticles go in the cell, a nuclear stain (Hoechst 33342) was used. A working solution of 1:2000 or 5 µg/ml was first prepared and then 1 ml of Hoechst was placed in the well in the dark. This solution was allowed to sit in the wells for 20 minutes. The rest of the work was conducted with minimal light to ensure that no stray ultraviolet light would excite the stain and cause it to degrade prematurely. Excess Hoechst 33342 was removed from the well and the cells washed another three times with sterile PBS. Next a small amount of glycerol was placed on a glass slide and the glass cover that contained the fixed and stained cells was mounted onto the glass slide. A small amount of nail polish was applied to the edges of the glass slip cover to secure it to the glass slide.

The control cells (no treatment) were fixed and stained at the same time as the 48 hour cells. This experiment was performed in triplicate with the cells being trypsinized between each batch and all the slides were then viewed under the laser scanning confocal microscope under 60x oil immersion magnification (NA:1.40) with the z projections showing 18 slices at 0.30 µm thick on a Olympus Fluoview FV1000 (Tokyo, Japan).

ImageJ, Adobe Photoshop, Olympus Fluoview 3.0 software, and excel were employed for image and statistical analysis.

2.7 Evaluation of Transfection of Chitosan/siRNA Nanoparticles Using Live Cell Imaging

Cells grown on glass coverslips were placed in a Delta T culture dish (Bioptechs) that is modified to work with the Delta T heated stage adapter (Biotechs, Butler, PA, USA) for the Olympus Fluoview Fv1000 laser scanning confocal microscope. Lipofectamine 2000/siRNA and chitosan/siRNA solutions were then prepared at a concentration of 100 nmol/ml. The cells were submerged in 10% FBS and antibiotic supplemented DMEM then imaged using an Olympus 20x water objective lens (NA: 0.95) as a control. Then the media was replaced with 500 µl of transfection media (Lipofectamine 2000/siRNA or chitosan/siRNA nanoparticles). The movement of the siRNA across the cell membrane was monitored over time. The settings for taking the images were not the same for the Lipofectamine 2000/siRNA or the chitosan/siRNA but they are listed in the figure captions.

CHAPTER III

RESULTS

3.1 Evaluation of siRNA Loading Efficiency

The loading efficiency of siRNA into the chitosan and the chitosan-PEG nanoparticles were determined in order to know the concentration of siRNA that will be used with the colorectal cancerous cells. As stated previously a ladder was constructed using various known concentrations of siRNA and three concentrations were chosen that represent the absorbances closest to the unknown absorbance of unassociated siRNA (Figure 2). A trend line was then applied to the graph and the equation of the line was

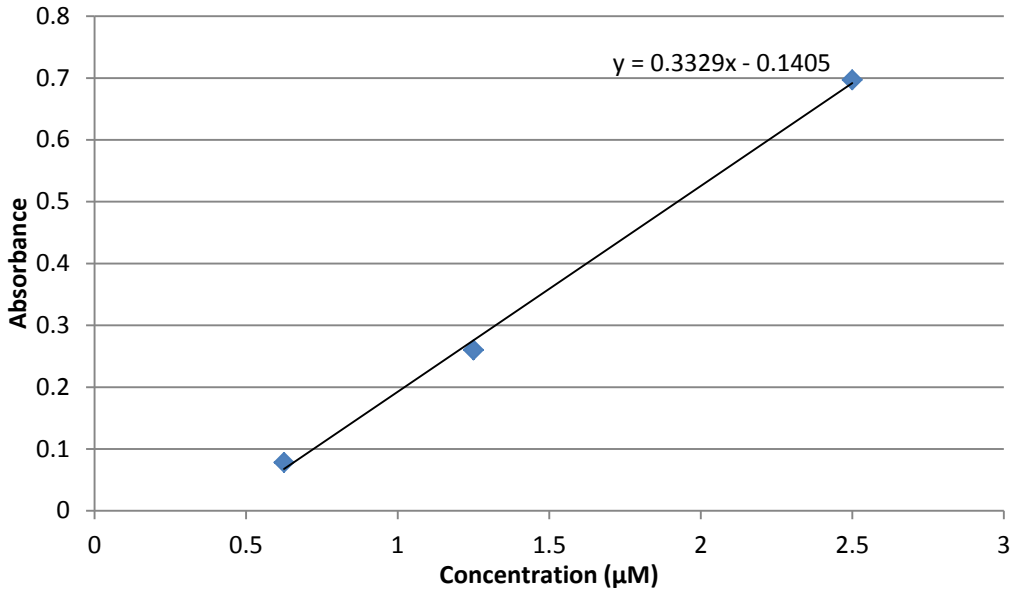

Figure 2. Absorbance as a Function of siRNA Concentration.

then determined. The equation was then used to find the concentration of unassociated siRNA in the supernatant of chitosan/siRNA and chitosan-PEG/siRNA nanoparticles. The supernatant from the chitosan nanoparticles was used as a blank before any absorbance measurements that were taken of the other supernatants. Three readings on each prepared nanoparticle batch were averaged to determine the percent encapsulation. For three different batches of the chitosan/siRNA nanoparticles, 83% of siRNA was associated with the nanoparticles. For two batches of the chitosan-PEG/siRNA nanoparticles, 88% of siRNA was associated with the nanoparticles.

3.2 TEM Characterization of Nanoparticles

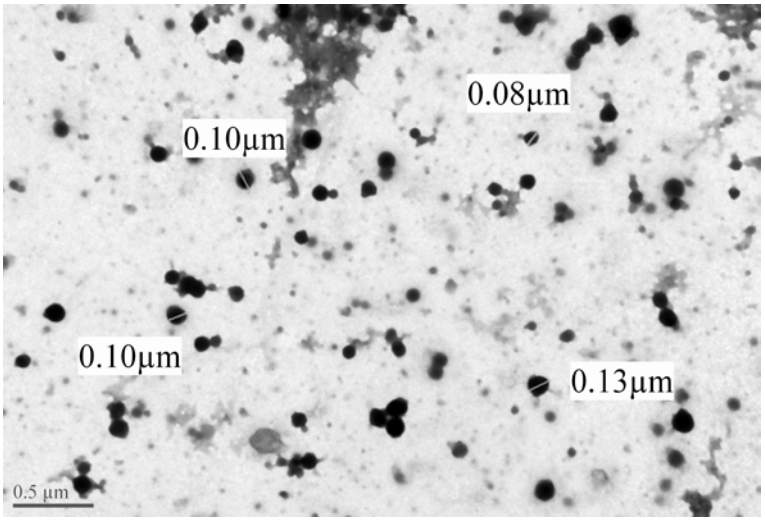

Figure 3. **TEM Image of Chitosan Nanoparticles.** Size and morphology of chitosan nanoparticles at 40K magnification.

The size and morphology of chitosan and chitosan/siRNA nanoparticles were evaluated using several different techniques. Figure 3 shows a TEM image of the chitosan nanoparticles. The image shows a representative sampling of the size of these nanoparticles ranges from about 80 nm to 130 nm in diameter with a generally spherical shape. Figure 4 is a TEM image of chitosan/siRNA nanoparticles. The morphology of the

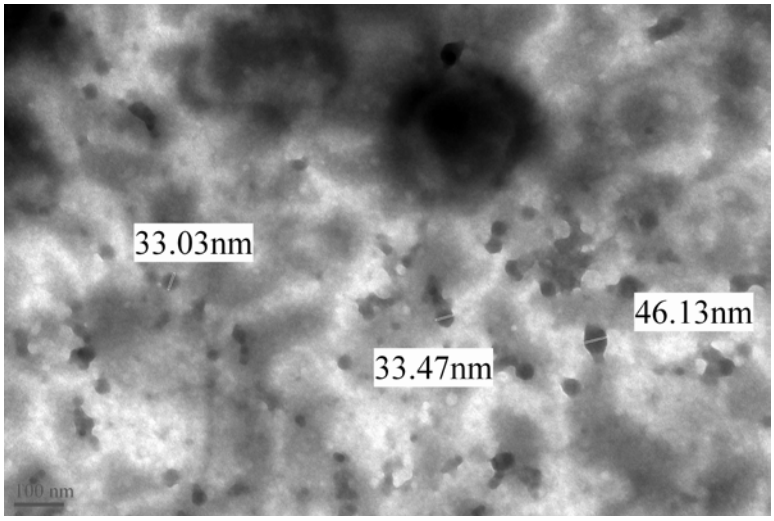

Figure 4. TEM Image of Chitosan/siRNA Nanoparticles. Size and morphology of the chitosan/ siRNA nanoparticles at 120K magnification.

chitosan containing siRNA is spherical and a representative sampling of the size of the nanoparticles indicates a size range from 33 nm to 46 nm. The chitosan/siRNA nanoparticles containing siRNA are generally smaller than the chitosan nanoparticles that do not contain siRNA.

3.3 SEM and EDS Characterization of Nanoparticles

Next chitosan and chitosan/siRNA nanoparticles were visualized with a SEM to

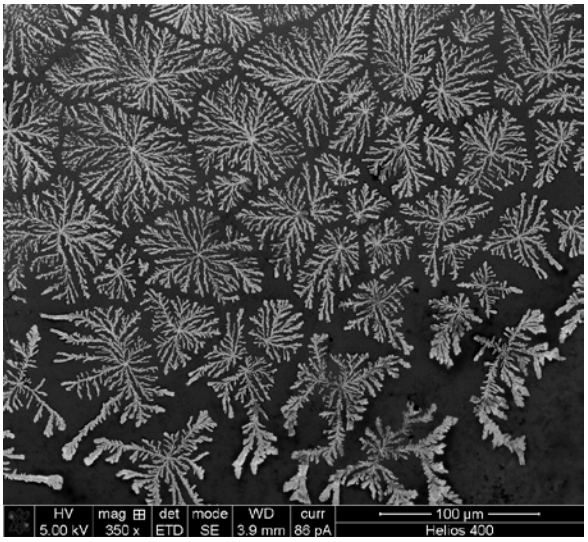

Figure 5. SEM Image of Chitosan/siRNA Nanoparticles at Low Magnification. Labels on image indicates settings used while image was taken.

further confirm size and morphology. Figure 5 shows chitosan/siRNA nanoparticles at low magnification. Notice that the particles appear as large dendritic branches, but upon closer inspection, small spherical particles can be discerned. This pattern appeared for

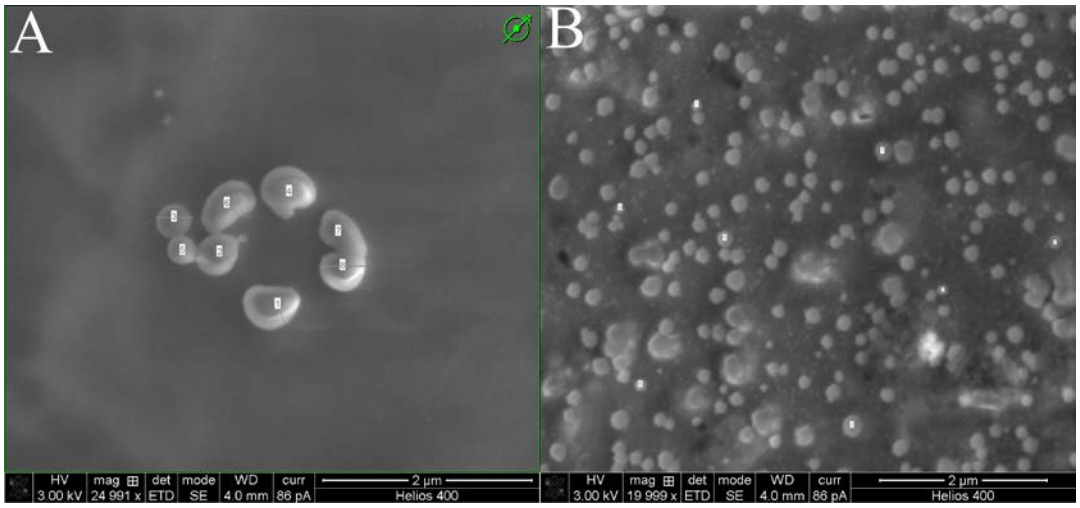

Figure 6. SEM Characterization of Nanoparticles. SEM image of ImageJ size analysis of chitosan (A) and chitosan/siRNA (B) nanoparticles. Labels indicate settings used to image.

both chitosan and chitosan/siRNA nanoparticles. Chitosan nanoparticles at a greater magnification can be seen in Figure 6 (A), and chitosan/siRNA nanoparticles can be seen in Figure 6 (B). Both figures show a morphology that is spherical and there is a size

Table 1. ImageJ Size Analysis. ImageJ size analysis from SEM image of chitosan and chitosan/siRNA nanoparticles. Data from Figure 6.

Table 1			
Chitosan	Diameter (nm)	Chitosan/siRNA	Diameter (nm)
1	373	1	116
2	368	2	121
3	350	3	133
4	474	4	119
5	269	5	165
6	339	6	129
7	325	7	219
8	430	8	226
Mean	366	Mean	153
SD	63	SD	45
Min	269	Min	116
Max	474	Max	226

difference between the two samples which is consistent with the data obtained from the TEM. Table 1 shows the measurement analysis that ImageJ performed on a random selection of nanoparticles labeled in Figures 6(A) and 6(B). There is a notable size difference between chitosan and chitosan/siRNA nanoparticles and Figure 7 shows the difference in the mean diameter when calculated using the data from Table 1 from the

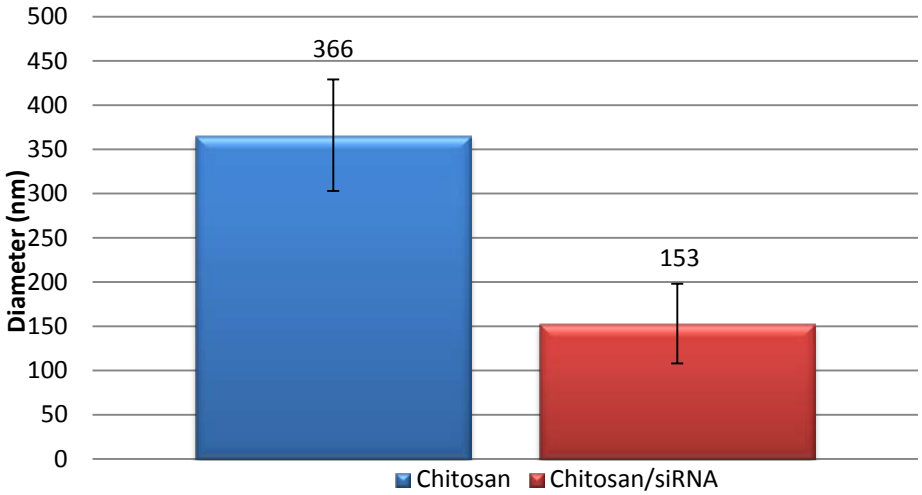

Figure 7. SEM Average Size of Nanoparticles. Average size of chitosan and chitosan/siRNA nanoparticles from SEM image as analyzed by ImageJ.

two types of nanoparticles.

EDS analysis was also taken of both types of nanoparticles. Figure 8 A is the chitosan nanoparticle spectrum and B is the chitosan/siRNA nanoparticle spectrum. Notice there is a relative difference between the carbon, oxygen, and nitrogen peaks when comparing the two spectra. Tables 2 and 3 show the elemental quantification of the chitosan and chitosan/siRNA nanoparticles taken from the EDS spectra. Here it can be seen that the molar ratio (atomic percent) between carbon to nitrogen (19) goes down when going from unencapsulated chitosan nanoparticles (Table 2) to encapsulated chitosan/siRNA nanoparticles (Table 3) where the ratio is 2.6. This would be expected when adding siRNA to a particle because siRNA introduces more nitrogen.

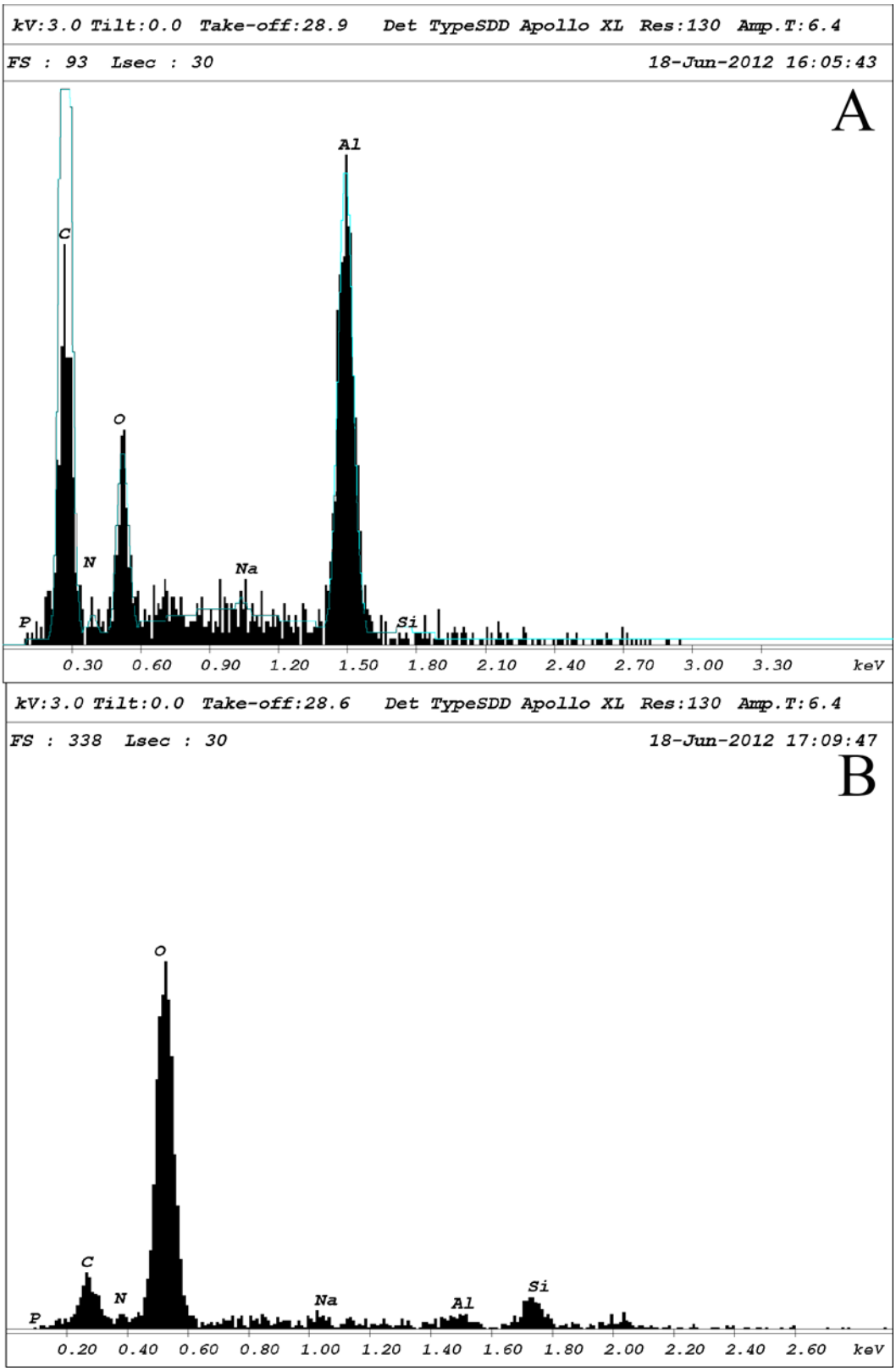

Figure 8. EDS of Nanoparticles. EDS spectra of chitosan (A) and chitosan/siRNA (B) nanoparticles. The main elemental characteristic peaks (K α lines) are labeled.

Table 2. EDS Quantification of Chitosan Nanoparticles. Elemental quantification of nanoparticles (data from Figure 7A).

Table 2				
Element	Weight %	Atomic %	Net Int.	Net Int. Error
C	22.26	37.3	14.71	0.05
N	1.36	1.95	0.6	0.81
O	6.89	8.67	5.62	0.14
Na	1.77	1.55	1.43	0.69
Al	67.72	50.52	22.48	0.05

Table 3. EDS Quantification of Chitosan/siRNA Nanoparticles. Elemental quantification of nanoparticles (data from Figure 7B).

Table 3				
Element	Weight %	Atomic %	Net Int.	Net Int. Error
C	9.01	13.44	7.8	0.07
N	4.03	5.16	2.36	0.15
O	53.21	59.62	53.1	0.03
Al	9.01	5.99	3.49	0.13
Si	24.73	15.79	5.81	0.1

3.4 Dynamic Light Scattering Analysis of Nanoparticles

Table 4. DLS Size Analysis. A comparison of the size of chitosan and chitosan/siRNA nanoparticles by DLS analysis.

Table 4				
	Chitosan (d.nm)	Polydispersity index	Chitosan/siRNA (d.nm)	Polydispersity index
1	612	0.604	309	0.327
2	226	0.371	264	0.348
3	429	0.238	261	0.294
4	424	0.238	253	0.246
5	434	0.246	258	0.228
Mean	425		269	
SD	122		20	
Min	226		253	
Max	612		309	

Dynamic light scattering (DLS) was also used to compare the sizes of chitosan and chitosan/siRNA nanoparticles. For each batch, measurements were taken two to three times and the numbers averaged. Table 4 shows the results for the size analysis and Figure 9 compares the average for the two different nanoparticles. There is a significant size difference between these measurements and the measurements taken from the TEM and SEM. However, the data shows that the size of the chitosan/siRNA nanoparticles are always smaller than that of the chitosan nanoparticles.

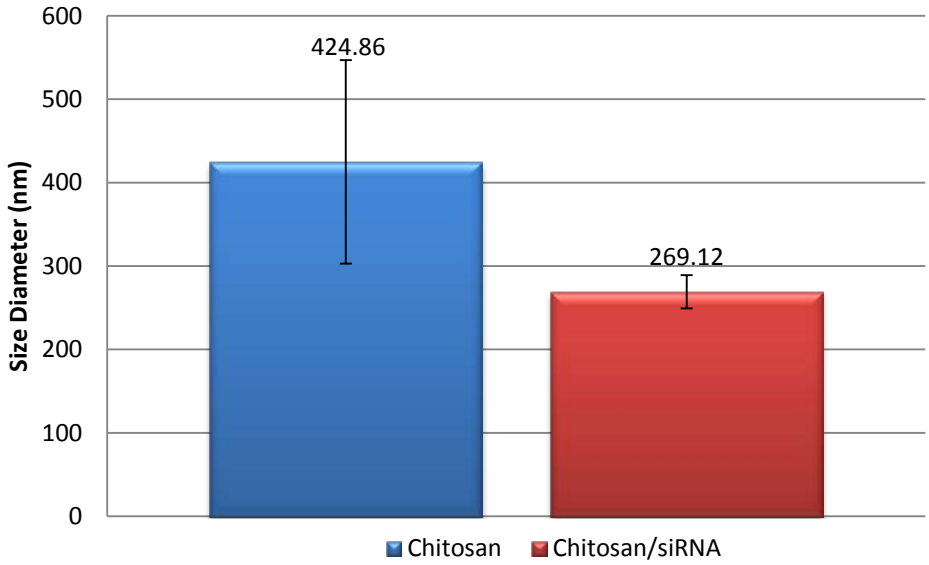

Figure 9. DLS Average Size of Nanoparticles. Average size of chitosan and chitosan/ siRNA nanoparticles from dynamic light scattering analysis (data obtained from Table 4).

3.5 Confocal Microscopy Characterization of Nanoparticles

Under a 60x oil immersion lens, the grids from the TEM were placed under the confocal microscope. The same laser settings were used to capture images for both chitosan and chitosan /siRNA nanoparticles. Figure 10 (A) shows chitosan under these conditions, and there is no fluorescent signal. When the grid from chitosan/siRNA is viewed under the same conditions, an abundance of red fluorescence can be seen (Figure 10 B). The red fluorescence of the chitosan/siRNA is also clumped together in the same

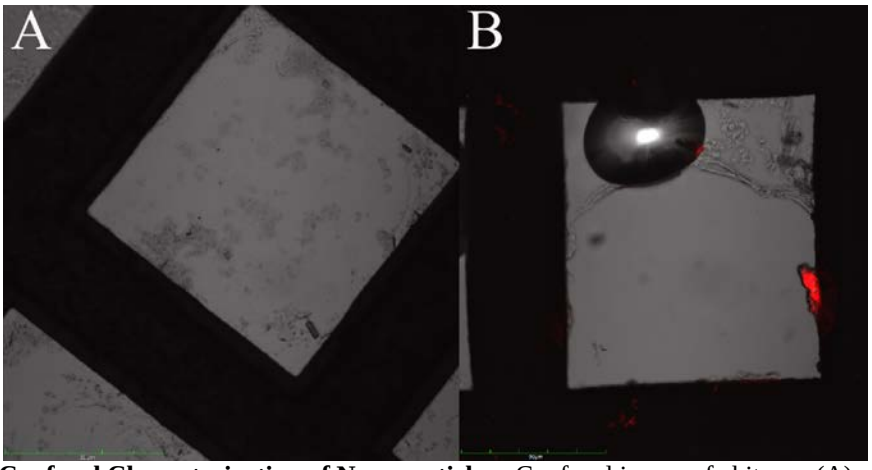

Figure 10. Confocal Characterization of Nanoparticles. Confocal image of chitosan (A) and chitosan/siRNA (B). The red is the fluorescently labeled siRNA with AlexaFluor 555. Images show the entire z projection with 18 slices at 0.30 µm thick. Scale bars are 50 µm.

manner as the nanoparticles were when viewed at higher magnification on the SEM (Figure 5). This demonstrates that the fluorescently labeled siRNA is associated with the chitosan/siRNA nanoparticles.

3.6 Evaluation of Transfection of siRNA Nanoparticles Using Laser Scanning Confocal Microscopy

As stated previously, transfection into HCT 116 cells by all three delivery vehicles (Lipofectamine 2000/ siRNA, chitosan/siRNA, and chitosan-PEG/siRNA nanoparticles) was stopped at certain time intervals via fixation of the cells and visualized under 60x oil immersion magnification (NA: 1.40) under the confocal microscope. The same settings were used to image every slipcover including the controls and the z projection is shown in every image with 18 slices at 0.30 µm thick. The siRNA was fluorescently labeled with AlexaFluor 555 (red) while the cell nuclei were stained with Hoechst 33342 (blue) nuclear stain. Cells fixed at 12 hours, 24 hours, and 48 hours post transfection were visualized and imaged along with cells that received no treatment (negative control). This was done for all three delivery vehicles.

Control

The cells that did not receive any treatment were fixed with 4% paraformaldehyde 48 hours after the cells treated with the nanoparticles. Figure 11 shows the outcome of these non-treated cells: (A) shows the cells with the nuclei stained blue from the Hoechst stain with all the channels showing including the transmitted light, (B) shows the cells

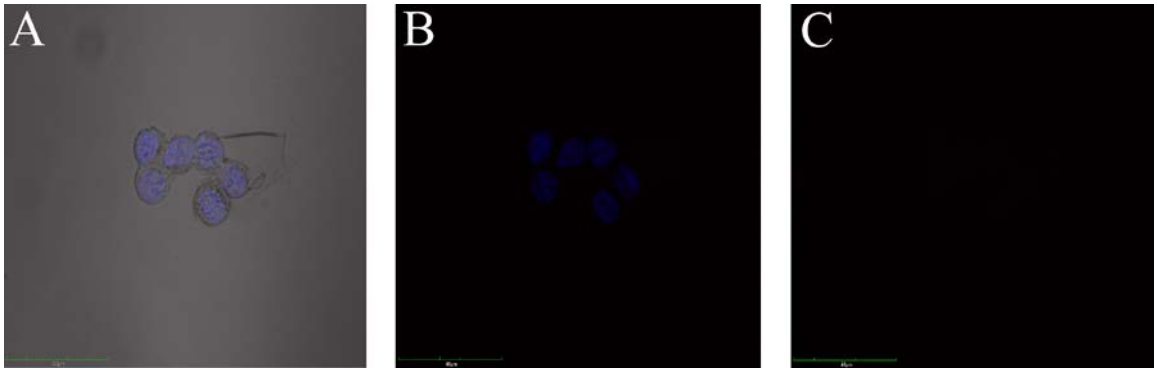

Figure 11. Control Cells. HCT 116 control cells show blue nuclei stained with Hoechst 33342 nuclear stain with all channels showing (A), with only red and blue channels showing (B), and with only the red channel showing (C). The entire z projection is shown with 18 slices at 0.30 µm thick. The scale bars are at 40 µm.

with the blue nuclei and the red channel without transmitted light, and (C) shows only the red channel. As can be seen in (C), there is no red fluorescence showing, thus confirming that these cells did not contain the fluorescent siRNA and the cells are not auto-fluorescing in the red channel. This was done for each batch of experiments although only one example is shown here.

Figure 11 (C)s image was then taken and its histogram in the red channel viewed (Figure 12). Histograms are used here to generate a numerical profile of fluorescence intensity so that any fluorescence not seen due to printing and/or resolution inadequacies can still be considered. The x axis is the pixel intensity where 0 represents black pixels and the other end represents white pixels. The y axis is the pixel frequency or the number of pixels for any given intensity. What Figure 12 shows is that there is quite a few of dark

or black pixels (ranging from 28 to 64) that can be observed. This is consistent with the image and what is expected if the cells did not receive any treatment.

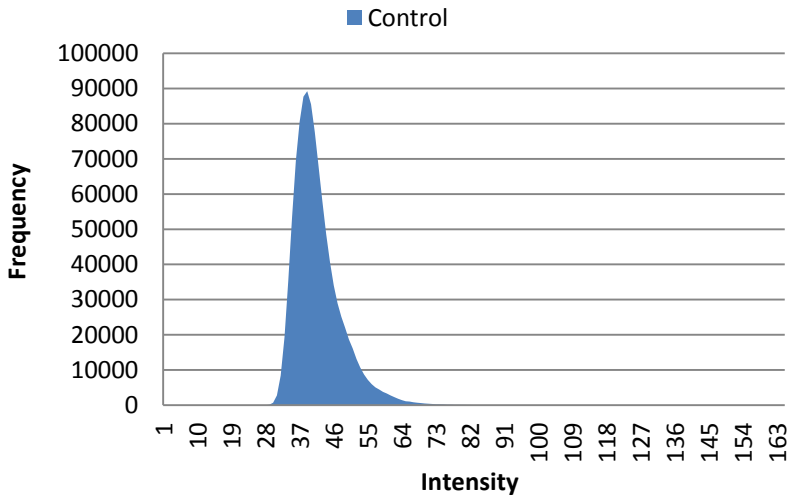

Figure 12. Histogram of Control Cells. Red channel histogram of HCT 116 control cells that did not contain any fluorescent siRNA. Data obtained from Figure 11 C.

12 Hours Post Transfection

12 hours post transfection one slipcover from each type of treatment was fixed and stained. Figure 13 shows the results. Again the blue corresponds to nuclei stained with Hoechst 33342 nuclear stain and the red corresponds to the AlexaFluor 555 fluorescent labeled siRNA. The first row shows the Lipofectamine 2000/siRNA (positive control) treatment, the second row shows the chitosan/siRNA treatment and the third row shows the chitosan-PEG/siRNA treatment. The first column shows the image with all the channels displayed together, the second column shows only the blue and red channels, and the third shows only the red channel so that the red fluorescent siRNA can be better distinguished. The Lipofectamine 2000 treatment does show a significant amount of fluorescence when compared to the other two chitosan based treatments, while the chitosan based treatments demonstrate a very similar fluorescence to each other at this point in time. The chitosan and chitosan-PEG treatments have a fluorescence signal that

seems to be evenly distributed, while the Lipofectamine treatment has its fluorescence concentrated in certain spots within the cell's cytoplasm.

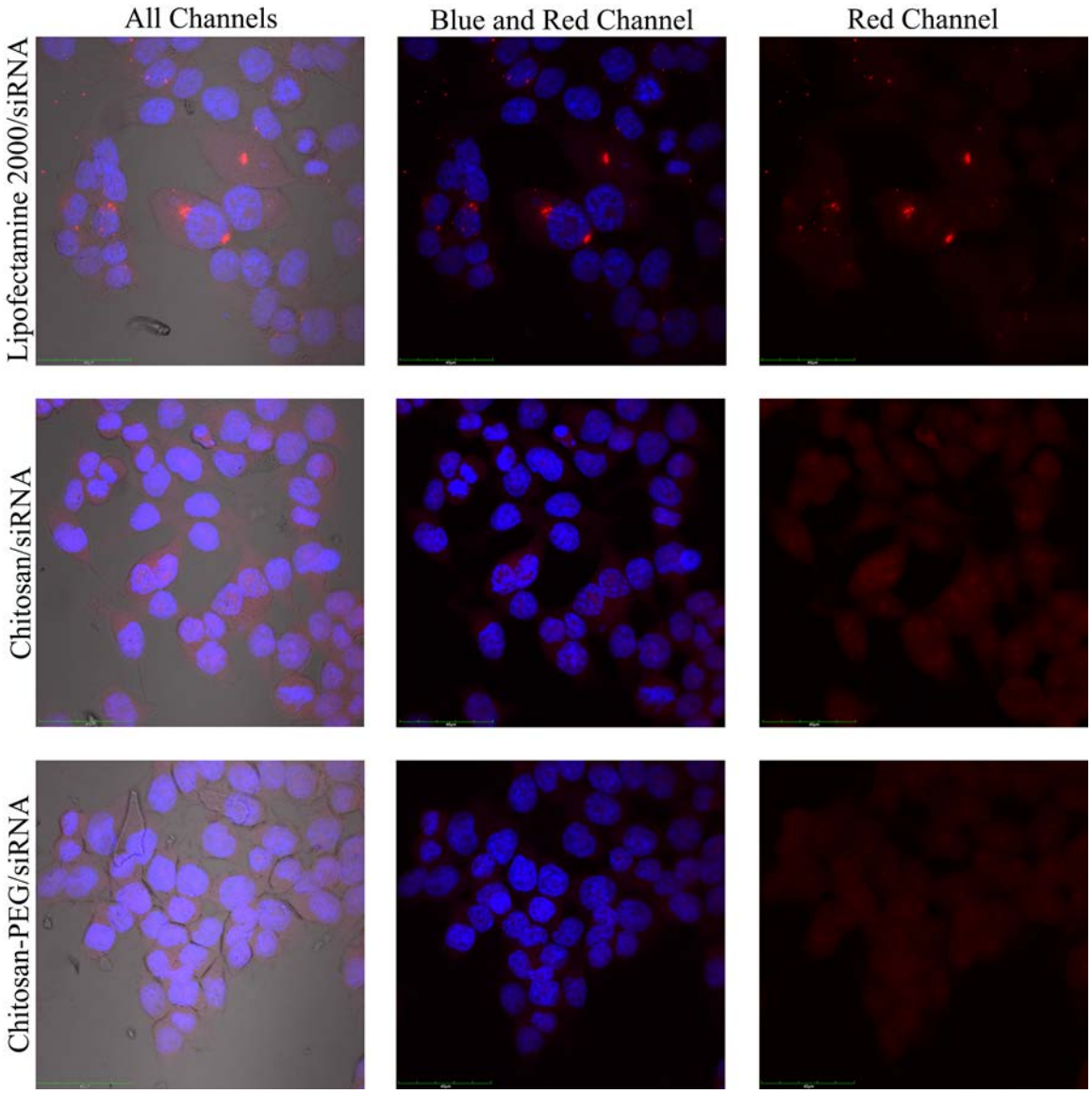

Figure 13. 12 Hours Post Transfection. HCT 116 cells nuclei stained with Hoechst 33342 (blue) 12 hours post transfection with siRNA (AlexaFluor 555 red) encapsulated within three different delivery vehicles. First row corresponds with the Lipofectamine 2000/siRNA, second row the chitosan/siRNA and the third row the chitosan-PEG/siRNA treatment. The first column shows an image with all channels visible, the second column has only the blue and red channels displayed, and the third column only displays the red channel. All images show the full z projection with 18 slices at 0.30 µm thick. Scale bars are at 40 µm.

Figure 14 shows the results for the three images in the red channel column from Figure 13. Ignoring the fluorescent intensity between 30 and 88 which is due to

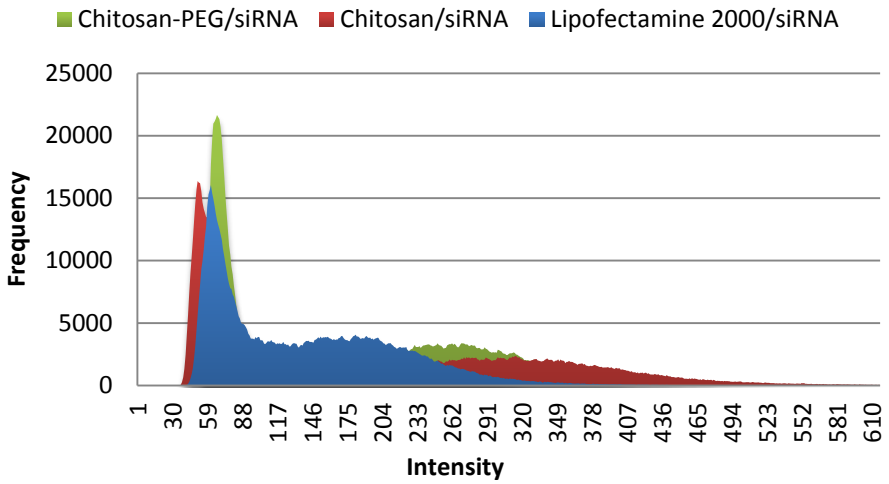

Figure 14. Histogram of 12 Hours Cells. Histogram of the red channel of the images from Figure 12 red channel column overlaid on each other.

background, this histogram shows that Lipofectamine 2000/siRNA (blue) generates a higher frequency than either of the chitosan based treatments when comparing the second peaks. It also shows that the chitosan-PEG/siRNA treatment generates a higher frequency at a fluorescent intensity level of 270 than the chitosan treatment which has a slightly lower frequency at its peak maximum fluorescent level of 330.

The images in Figure 13 do show the amount of fluorescence associated with the cells but what they do not show is if the fluorescence is originating from the cell's cytoplasm or from the cell surface. In order to visualize this, images were turned on their x axis to show the distribution throughout the thickness of the cells. Figure 15 shows the cells rotated on the x axis. These images indicate that the fluorescence has penetrated the cellular membrane and is distributed throughout the cytoplasm. Large amounts of streaking of the fluorescence can be seen in part A due to the clustering as a result of the Lipofectamine 2000 treatment while a more dispersed fluorescence is found in the

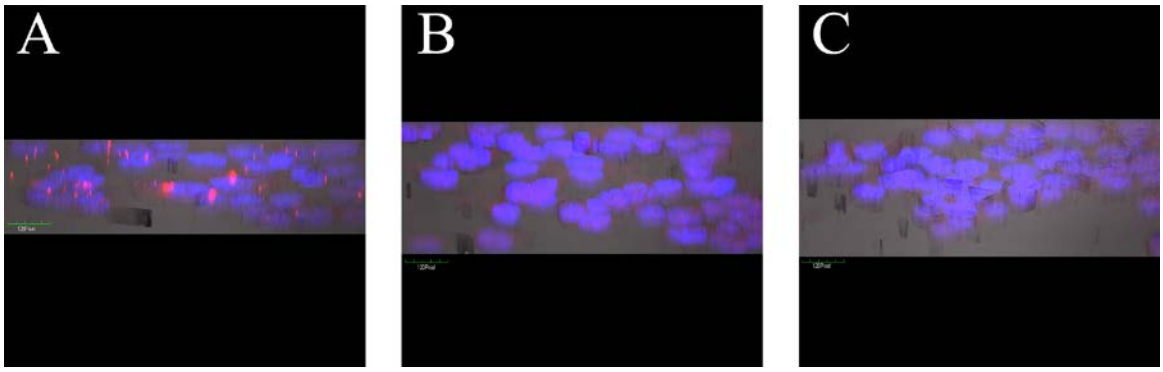

F**igure 15. 12 Hour Cells Turned on X Axis.** Figure 11 cells were turned on their x axis. (A) is Lipofectamine 2000/siRNA, (B) is chitosan/siRNA, and (C) is chitosan-PEG/siRNA (siRNA is red from AlexaFluor 555 tag). The nuclei are stained with Hoechst 33324 (blue). Scale bars are 120 pixels.

chitosan based nanoparticles (B and C). This confirms that the nanoparticles are indeed transfecting across the cell's membrane and dispersing throughout the cytoplasm.

24 Hours Post Transfection

Figure 16 shows the cell line 24 hours post transfection of the three different treatments. The first row shows the Lipofectamine 2000 treatment, the second row shows the chitosan treatment, and the third row shows the chitosan-PEG treatment. The first column displays all the channels, the second column displays only the blue and red channel, while the third column displays only the red channel. As can be seen in the figure, the siRNA appears close to the nuclei indicating that the siRNA is within the cell's cytoplasm. The tagged siRNA also appears in clumps because there are certain spots within the cytoplasm that are brighter than others. The Lipofectamine 2000 treatment does contain more of the clusters and has a higher intensity of siRNA fluorescence. This indicates that more siRNA transfected across the plasma membrane than in either of the chitosan based delivery vehicles. There also is a slight difference between the chitosan/siRNA and the chitosan-PEG/siRNA. The chitosan-PEG treatment

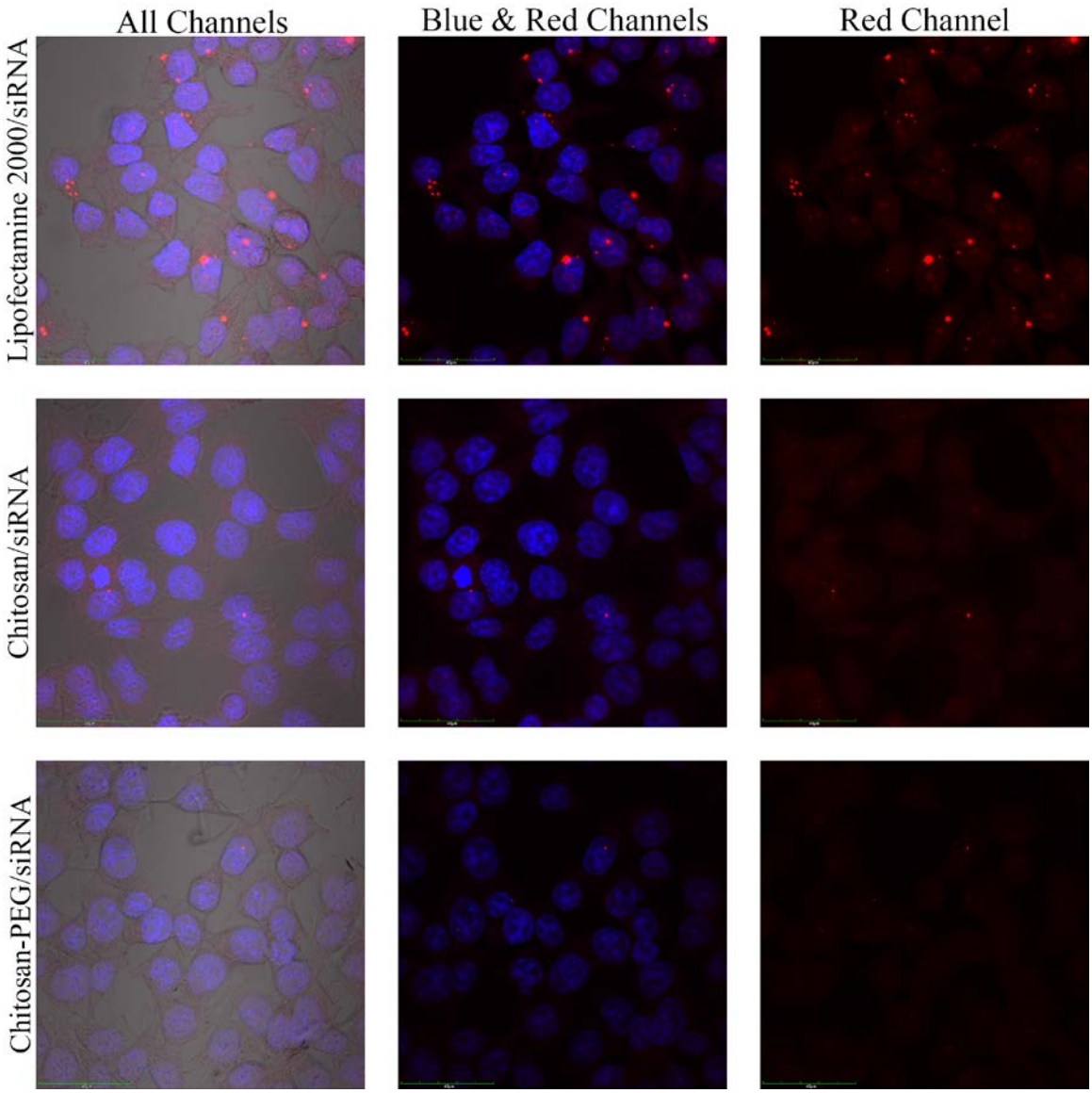

Figure 16. 24 Hours Post Transfection. HCT 116 cells with nuclei stained with Hoechst 33342 (blue) 24 hours post transfection with siRNA (AlexaFluor 555 red) in three different delivery vehicles. First row corresponds with the Lipofectamine 2000/siRNA, second row the chitosan/siRNA and the third row the chitosan-PEG/siRNA treatment. The first column shows an image with all channels visible, the second column has only the blue and red channel displayed, and the third column only displays the red channel. The z projection is shown with18 slices at 0.30 µm thick. Scale bars are at 40 µm.

has slightly more clusters than the chitosan treatment even though the intensity of fluorescence appears lower.

When the histograms of all three treatments are compared to each other a similar trend can be seen (Figure 17). The first observation that can be made from the histogram

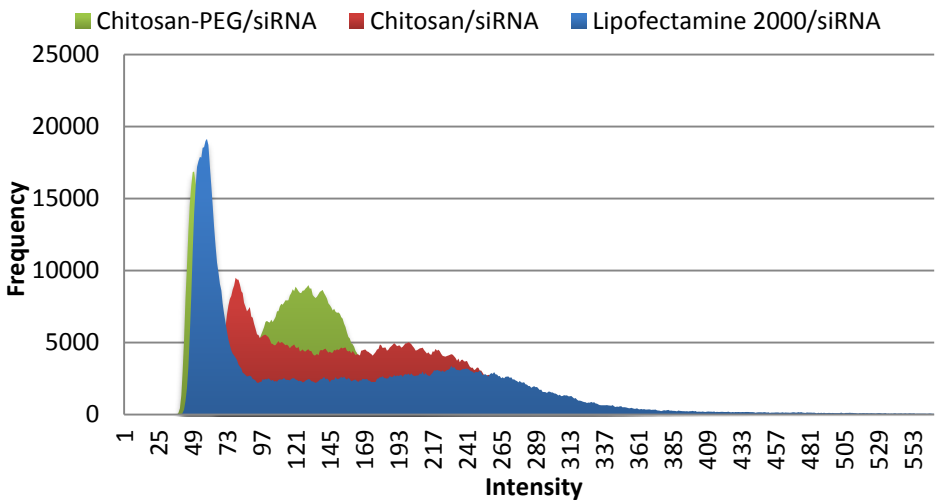

Figure 17. Histogram of 24 Hour Cells. Histogram of the red channel of the images from Figure 15 red channel column overlaid on each other.

is that the majority of the intensity is lower than in Figure 14. Secondly the frequency for the chitosan-PEG/siRNA is higher than that of the chitosan/siRNA nanoparticles. Thus both observations about the siRNA coming together in clusters and the chitosan-PEG treatment generating more clusters have supporting evidence with the histograms. Although the intensity of the fluorescence is lower, the frequencies are higher. This may be due to the fact that there could be several lower fluorescent intensities close together that give the visual perception of one bright fluorescent intensity. It is attributed to the fact that the human eye cannot resolve as much as the detector can in this case.

48 Hours Post Transfection

When the cells were fixed 48 hours post transfection of the treatments, a continuation of the previously observed trends appears (Figure 18). Using the same confocal microscopy settings as used to visualize the previous cells, the fluorescently-labeled siRNA (red) can be observed along with the nuclei stained with Hoechst 33342 (blue). The labels for the columns and the rows are the same as in Figure 13. The fluorescence appears to be in all areas of the cytoplasm; however the density of the

fluorescence appears to be more clustered than that of the cells fixed 12 hours and 24 hours post transfection of the treatments. The fluorescence frequency difference between the chitosan and the chitosan-PEG treated cells is very hard to determine visually in these images so the histograms will be needed for further evaluation.

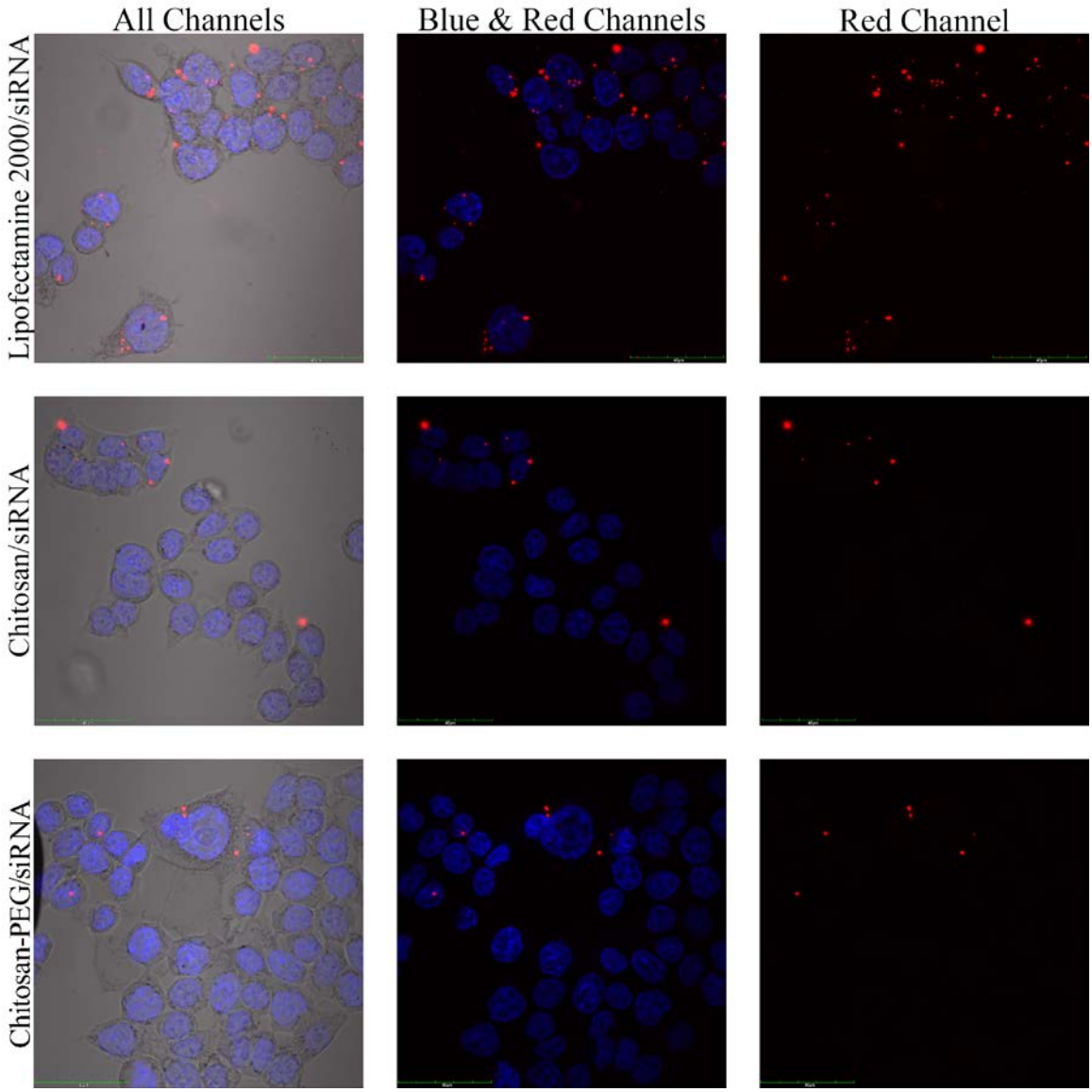

Figure 18. 48 Hours Post Transfection. HCT 116 cells 48 hours post transfection with fluorescently labeled siRNA (AlexaFluor 555 red) and nuclei stained with Hoechst 33342 (blue) in three different delivery vehicles. First row corresponds with the Lipofectamine 2000/siRNA, second row the chitosan/siRNA and the third row the chitosan-PEG/siRNA treatment. The first column shows an image with all channels visible, the second column has only the blue and red channels displayed, and the third column only displays the red channel. All of the z projection is shown with 18 slices at 0.30 µm thick. Scale bars are at 40 µm.

Figure 19 shows the red channel histogram of Figure 18's red channel column. From the figure it can be seen that the frequency of the red channel in the chitosan/siRNA is higher than the frequency in the red channel for the chitosan-PEG/siRNA. However the intensity in the chitosan-PEG is slightly higher than that of the chitosan. Meaning that there are more black pixels (or less red fluorescence) from the cells with the chitosan treatment than that of the cells with the chitosan-PEG treatment. What is interesting is

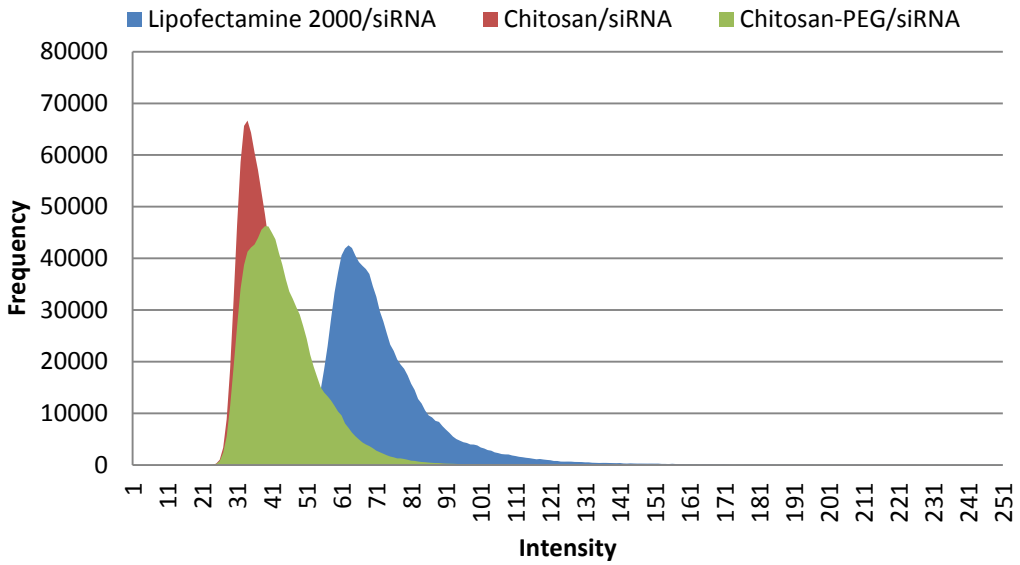

Figure 19. **Histogram of 48 Hour Cells.** Histogram of the red channel of the images from Figure 17 red channel column overlaid on each other.

that all of the histograms in this figure look very similar to the control cells histogram. This is expected since the number of black pixels is increasing as the clustering takes place and as the cells divide fluorescence will be lost. Although the histograms for these images did aid in identification of trends, quantitative results will be needed to help distinguish which of the chitosan treatments (chitosan/siRNA or chitosan-PEG/siRNA) has the best transfection efficiency.

3.7 Evaluation of Transfection of Chitosan/siRNA Nanoparticles Using Live Cell Imaging

Lipofectamine 2000/siRNA and chitosan/siRNA were both visualized during the four hours that the transfecting media is allowed to incubate with the cells on the confocal with a 20x water lens (NA: 0.95) magnification. The Lipofectamine treatment and the chitosan treatment did not use the same settings for visualizations so no quantitative data can be used to compare the two. However the images obtained by both treatments can be used to describe the behavior of the nanoparticles transfecting across the cellular membrane. In the supplementary materials (APPENDIX A), a video can be found that shows the transfection of Lipofectamine 2000/siRNA and the chitosan/siRNA. Although the videos cannot be shown on paper, a few of the images are shown below.

Figure 20 (A) is the final z stack taken after 60 minutes of transfection with the Lipofectamine 2000/siRNA. Four z stacks were taken prior to the one shown with 14

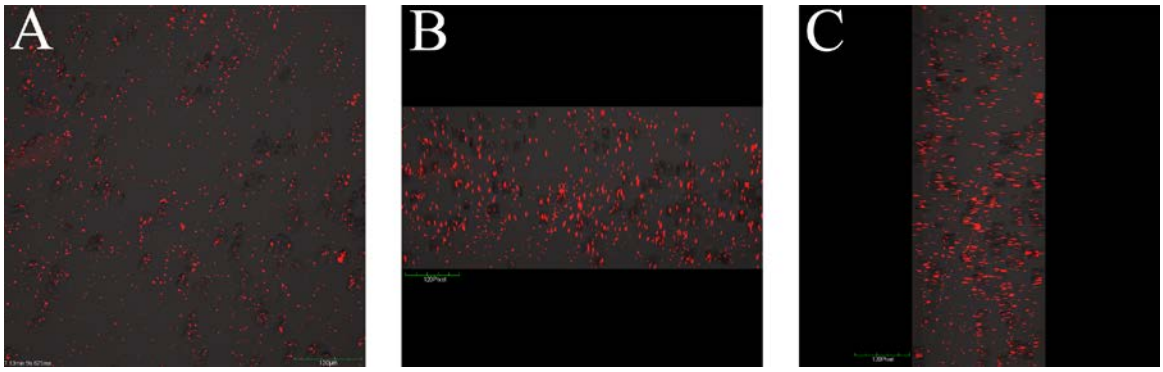

Figure 20. Lipofectamine 2000/ siRNA Live Cell Images. HCT 116 cells during live cell imaging taken 60 minutes after transfection with Lipofectamine 2000/siRNA (AlexaFluor 555 red) (A). The image was also turned on its x axis (B) and y axis (C) to visualize penetration of siRNA into the cell. (A) taken with a 20x water lens (NA: 0.95) with all z projection showing 14 slices at 1.5 µm thick. Scale bar is at 120 µm (A) and the digital projections (B & C) have a scale of 120 pixels.

slices at 1.5 µm thick. This image has the same slices and thickness. The next two images in the figure are digital projections of the same image turned on the x axis (B) and the y axis (C). The rotation of the image is required to see whether or not the fluorescence has penetrated the cellular membrane or not. The first observation about the image is that

there is ample fluorescence and it is dispersed enough to show the movement of the siRNA across the cellular membrane. When the images are rotated on the x and y axis it can be seen that some of the fluorescence can be found inside the cell while there are also areas of fluorescence that are associated with the cell but have not penetrated the cellular membrane. It looks as though small amounts of the fluorescence have penetrated the membrane while the majority of the fluorescence is not on the inside of the membrane.

Images obtained from the transfection of the chitosan/siRNA video are different.

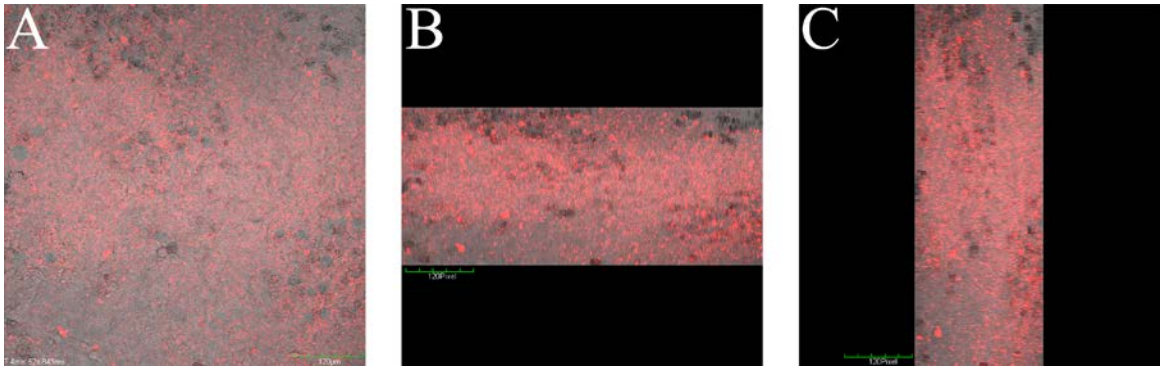

Figure 21. Chitosan/siRNA Live Cell Images. HCT 116 cells in transfection media containing chitosan/siRNA (AlexaFluor 555 red) nanoparticles. Images were taken 50 minutes after transfection media was added (A) and turned on its x (B) and y (C) axes. Taken with a 20x water lens objective with 12 slices at 1.0 µm thick. Scale bar is at 120 µm (A) and digital projections (B & C) have a scale of 120 pixels.

Figure 21 shows a confocal z stack taken 50 minutes after the addition of the chitosan/ siRNA transfection media to the dish containing the cells. The first image (A, taken last), shows the full z projection of 12 slices at 1.0 µm thick. This image shows the nanoparticles unevenly distributed throughout the media. Nanoparticles with extremely large sizes (>200nm) can be visualized even though the solution was ran through a 0.2 µm syringe filter for sterilization purposes. When the image was turned on the x and y axes visualizing the cells is difficult due to the presence of so much fluorescence. What can be seen is that there is very little fluorescence inside the cells; however, there appears to be an abundant amount of fluorescence associated with the outside of the cellular

membrane. The little fluorescence that has penetrated the cellular membrane appears to be less than the fluorescence found on the outside and around the cell membrane.

CHAPTER IV

DISCUSSION

Three types of nanoparticles were characterized throughout this project: chitosan, chitosan/siRNA, and chitosan-PEG/siRNA. Each nanoparticle has its own distinctive physiochemical properties. Four important questions were addressed in this work. Can small particles be prepared? Can we incorporate siRNA into these chitosan based nanoparticles? Lastly, do the chitosan based nanoparticles penetrate or transfect across the cellular membrane and into colon cancer cells and if so how efficiently?

4.1 Size

The size of the nanoparticles is very important because it greatly affects transfection efficiency. In several different studies, non-targeting vector-DNA complexes over several different cell lines were found to have optimal gene transfer when the average size diameter of the delivery vehicle (vector) was between 70 to 100 nm[7]. But how does one tailor the size of a nanoparticle? There is not just one answer for that question; however, there are several factors that affect overall size.

One important factor to consider is the order of addition of the gene delivery vehicle to the RNA or DNA. In other words, should the siRNA be added to the polymer or the polymer added to the siRNA? The reason why this is important is because the ultimate size and morphology are kinetically driven.[4] In our case small amounts of TPP, a crosslinking agent, and siRNA were added to an excess of chitosan solution very slowly.

This was done to insure that as much as possible of the negatively charged TPP and siRNA were exposed to the positively charged chitosan as possible. This approach then favors intramolecular binding of the chitosan as opposed to intermolecular bonding which would favor the formation of aggregates.

Another factor to consider is the method of preparation. As mentioned in the introduction, there are several methods to make chitosan particles. Katas and Alpar have shown that chitosan/ siRNA nanoparticles prepared using the ionic gelation method produce the smallest particles when compared to nanoparticles prepared using a simple complexation method.[23]

Solubility and aggregation of the chitosan solution are other factors to consider. Because of the degree of deacetylation (DD) in chitosan, one characteristic that is apparent is aggregation. One way to control this is the use of dilute acidic solutions below a pH of 6.0 to help with solubility. Other more mechanical methods, such as sonication and filtration, can also be employed throughout the preparation method to aid in solubility as well.

Finally, a chemical modification of chitosan by using polyethylene glycol (PEG, called pegylating) does impart an increased solubility of the chitosan solution. A solubility increase was seen visually when comparing the chitosan/siRNA nanoparticles to the chitosan-PEG/siRNA particle and by the evidence of loading efficiency. The chitosan/siRNA nanoparticles had only an 83% loading efficiency while the chitosan-PEG/siRNA nanoparticles had an 88% loading efficiency. Katas and Alpar also showed that size was smaller when using the cross linker TPP compared to nascent chitosan particles.[23]

After chitosan/siRNA particles and chitosan-PEG/siRNA nanoparticles were prepared using various techniques to control size, they next had to be characterized. TEM, SEM, and dynamic light scattering (DLS) were all applied to determine size. However, some of the results conflicted with each other. The results from the TEM showed chitosan/siRNA nanoparticles with a diameter ranging from 33 nm to 46 nm, while the SEM showed nanoparticles with an average diameter of 153 nm. The DLS results on the other hand showed an average diameter of 269 nm. Why such a big variation in size diameter? The answer maybe two fold: the size displayed depends on how the instrument interacts with the sample, and the sample may have contained a range of sizes.

TEM displays images of samples by bombarding samples with electrons on one end and collecting the electrons that pass though the samples on the other end. The varying shades of gray are produced by the amount of electrons that can penetrate the sample without being absorbed or scattered by the sample.[24] In order to modulate the electrons, vacuum conditions are employed. Chitosan is a perfect candidate to be imaged this way because it is cationic and can easily absorb electrons. TEM has the capability of producing highly resolved images at very high magnification. The TEM images here have the highest magnification when compared to SEM and DLS and can provide the greatest clarity on the sizes of the nanoparticles.

SEM also bombards a sample with electrons under vacuum conditions; however it constructs the image in a different manner. An image is constructed by taking the electrons that have backscattered off of the sample.[24] SEM has the capability of producing a highly resolved image of a surface of a sample at high magnification, but not

as high as TEM. In our case, SEM images seem to indicate a dendritic structure but on closer inspection, it is apparent that SEM is visualizing a number of pseudo-spherical nanoparticles that are in close contact. Another drawback with SEM is that the sample must be conductive and chitosan stores electrons since chitosan is cationic. This produces two separate effects: the electrons tend to destroy the chitosan, and electrons are not back-scattered to produce an image. These two effects are the reasons as to why the SEM did not image some of the smaller nanoparticles.

DLS works in a totally different manner. Samples in solution have a monochromatic light shined on them. This light then bends and refracts and with Brownian motion over time we can calculate the size of the particle as it moves through the solution. One assumption used in the equation of Brownian motion is that the particle of interest being measured is spherical. As seen earlier chitosan nanoparticles do have a tendency to aggregate in a vacuum setting (as TEM and SEM show); however the same is true for chitosan in solution. Figure 20 shows live cell imaging of the chitosan/siRNA nanoparticles in DMEM. Before addition of the nanoparticles to the culture dish, the nanoparticles were pushed through a 0.2 μm filter for sterilization purposes. This would seem to eliminate any particles that would be above this size range. However from live cell imaging, fluorescent nanoparticles with a diameter above 200 nm can be distinguished. This provides support that chitosan nanoparticles aggregate quickly while in solution and may be the reason why the DLS results are different than the TEM or SEM results.

Although the different characterization methods did show different results for sizing of the nanoparticles, it is interesting that the chitosan/siRNA nanoparticles are

always smaller than the chitosan nanoparticles themselves in all three characterization methods. This shows that siRNA tends to contract the chitosan after its incorporation.

4.2 Incorporation of siRNA

Is siRNA actually being loaded onto the nanoparticles? There are three different methods that confirm this. First, the absorption measured at 260 nm of the supernatant after siRNA loading is an indirect approach that can be used to determine loading efficiency. The assumption made is that the rest of the missing siRNA is encapsulated or complexed with the chitosan nanoparticle.

In addition, two direct methods of detecting the siRNA were employed. The first method was elemental analysis using EDS. EDS is based on the principle that the impact of an electron beam can cause an electron to leave a lower orbital and be replaced by an electron from a higher orbital with a concomitant release of an x-ray. So each x-ray is characteristic of the identity of an element. These x-rays can be detected and analyzed to give information about the elemental make-up of the sample.[24] For this project, EDS spectra were taken for chitosan and chitosan/siRNA nanoparticles and Tables 2 and 3 show the quantitative results from those spectra. When the ratio of carbon to nitrogen atomic percentage is determined for chitosan and compared to that of chitosan/siRNA, a drop from 19.1 to 2.6 occurs. The drop can be attributed to the addition of siRNA to the nanoparticle which would be expected since siRNA would be adding more nitrogen groups to the nanoparticle.

Finally, the other direct method of detection of the siRNA was with fluorescence microscopy. The siRNA contained a fluorescent tag (AlexaFluor 555) covalently bound on the 5’ end of the sense strand. This fluorescent siRNA was only added to the chitosan/

siRNA nanoparticles and not the chitosan. When each set of nanoparticles was viewed under the confocal microscope after visualization from the TEM, only the image that contained the chitosan/siRNA particles had red fluorescence. This confirmed that the chitosan contained the siRNA and that the AlexaFluor 555 fluorescent tag functioned.

4.3 Transfection of siRNA Via Chitosan Based Nanoparticles

The last two questions to address are: do the chitosan based nanoparticles transfect the siRNA across the cellular membrane and if so how efficient are the chitosan-based nanoparticles? These questions were answered using classic confocal techniques and live cell imaging.

Classic Confocal Evaluation: 12, 24, and 48 Hours Post Transfection

We compared cellular membrane transfection of fluorescently labeled siRNA using classic confocal with staining and fixation techniques by utilizing three different delivery vehicles: Lipofectamine 2000, chitosan, and chitosan-PEG. Lipofectamine 2000 is a cationic liposome that has been extensively investigated and is known to transfect siRNA effectively.[25] The disadvantage of using Lipofectamine 2000 is that it is highly toxic when used in vivo. Chitosan as previously stated has the advantage that it is non-toxic and can be modified to improve its efficacy. In this work Lipofectamine 2000 was used as a standard of comparison to evaluate transfection efficiency for the two chitosan based delivery vehicles. The results showed that all three delivery vehicles did transfect the fluorescently labeled siRNA; however, the Lipofectamine 2000 treatment still showed superior transfection efficiency when compared to the chitosan/siRNA and chitosan-PEG/siRNA nanoparticles. As far as the transfection efficiency between the two chitosan particles, a visual comparison of the images taken at 12, 24, and 48 hours from confocal

imaging was inconclusive. The only way to tell the difference would be to quantitate the fluorescence. Due to advances in image processing technology, quantitation can be done with the present images; however that is beyond the scope of this project. Future direction would be to use this technology to aid in quantitation and also the development of pegylation techniques.

One interesting observation can be made with all three delivery vehicles (Lipofectamine 2000, chitosan and chitosan-PEG); over time the fluorescence inside the cytoplasm becomes more localized. The fluorescence sources become more clustered and located very close to the nucleus of each cell. This may be an indication that the siRNA has escaped the endosome and is currently being used by the RISC complex. It makes logical sense that the RISC complex would be found near the nucleus from where the mRNA originates. The evidence though circumstantial does not indicate that this is happening but it could be used as the basis for further experimentation.

Live Cell Imaging Evaluation

The last method used to answer the above questions was live cell imaging. The advantage of using live cell imaging is it can be employed in order to assess the behavior of the nanoparticles in solution while the respective transfection media is incubating the cells. In this case, it gave us a wealth of information that could not be attained by classical confocal techniques. Specifically, conclusive evidence was provided that size does affect transfection efficiency. The smaller fluorescent nanoparticles transfected first and faster than the larger fluorescent nanoparticles; which held true for the Lipofectamine 2000 and chitosan/siRNA treatments. Secondly live cell imaging gave us evidence that rapid aggregation of chitosan affects transfection. Even after the chitosan/siRNA solution

was passed through a 0.2 µm filter, there were still fluorescent particles that looked larger than 200 nm. The fluorescence of the chitosan/siRNA nanoparticles also appeared very dense when compared to the fluorescence of the highly dispersed Lipofectamine 2000/siRNA nanoparticles. These observations may also be the reason why the chitosan/siRNA nanoparticles over a period of time generated a range of sizes when using the different characterization methods.

APPENDIX A

SUPPLEMENTAL MATERIALS

Lipofectamine 2000/siRNA Live Cell Imaging

Lipofectamine all together 3.15.12.wmv

Chitosan/siRNA Live Cell Imaging

Chitosan email.wmv

REFERENCES

(1) Fire, A.; Xu, S.; Montgomery, M. K.; Kostas, S. A.; Driver, S. E.; Mello, C. C. Potent and specific genetic interference by double-stranded RNA in Caenorhabditis elegans. *Nature* **1998**, *391*, 806.

(2) Aagaard, L.; Rossi, J. J. RNAi therapeutics: Principles, prospects and challenges. *Adv. Drug Deliv. Rev.* **2007**, *59*, 75-86.

(3) Morris, K. V.; Chan, S. W. -.; Jacobsen, S. E.; Looney, D. J. Small Interfering RNA-Induced Transcriptional Gene Silencing in Human Cells. *Science* **2004**, *305*, 1289-1292.

(4) Pack, D. W.; Hoffman, A. S.; Pun, S.; Stayton, P. S. Design and development of polymers for gene delivery. *Nature Reviews Drug Discovery* **2005**, *4*, 581-593.

(5) Zhang, S.; Zhao, Y.; Zhi, D.; Zhang, S. Non-viral vectors for the mediation of RNAi. *Bioorg. Chem.* **2012**, *40*, 10-18.

(6) Rao, M.; Sockanathan, S. Molecular mechanisms of RNAi: Implications for development and disease. *Birth Defects Research Part C: Embryo Today: Reviews* **2005**, *75*, 28-42.

(7) Mintzer, M. A.; Simanek, E. E. Nonviral vectors for gene delivery. *Chem. Rev.* **2008**, *109*, 259-302.

(8) Varkouhi, A. K.; Lammers, T.; Schiffelers, R. M.; van Steenbergen, M. J.; Hennink, W. E.; Storm, G. Gene silencing activity of siRNA polyplexes based on biodegradable polymers. *European Journal of Pharmaceutics and Biopharmaceutics* **2011**, *77*, 450-457.

(9) Mao, S.; Sun, W.; Kissel, T. Chitosan-based formulations for delivery of DNA and siRNA. *Adv. Drug Deliv. Rev.* **2010**, *62*, 12-27.

(10) Tan, M. L.; Choong, P. F. M.; Dass, C. R. Cancer, chitosan nanoparticles and catalytic nucleic acids. *J. Pharm. Pharmacol.* **2009**, *61*, 3-12.

(11) Saranya, N.; Moorthi, A.; Saravanan, S.; Devi, M. P.; Selvamurugan, N. Chitosan and its derivatives for gene delivery. *Int. J. Biol. Macromol.* **2011**, *48*, 234-238.

(12) Tiyaboonchai, W. Chitosan nanoparticles: a promising system for drug delivery. *Naresuan University Journal* **2003**, *11*, 51-66.

(13) Dash, M.; Chiellini, F.; Ottenbrite, R. M.; Chiellini, E. Chitosan—A versatile semi-synthetic polymer in biomedical applications. *Progress in Polymer Science* **2011**, *36*, 981-1014.

(14) Csaba, N.; Köping-Höggård, M.; Alonso, M. J. Ionically crosslinked chitosan/tripolyphosphate nanoparticles for oligonucleotide and plasmid DNA delivery. *Int. J. Pharm.* **2009**, *382*, 205-214.

(15) Lai, W.; Lin, M. C. Nucleic acid delivery with chitosan and its derivatives. *J. Controlled Release* **2009**, *134*, 158-168.

(16) Dodane, V.; Vilivalam, V. D. Pharmaceutical applications of chitosan. *Pharm. Sci. Technol. Today* **1998**, *1*, 246-253.

(17) Park, J. H.; Saravanakumar, G.; Kim, K.; Kwon, I. C. Targeted delivery of low molecular drugs using chitosan and its derivatives. *Adv. Drug Deliv. Rev.* **2010**, *62*, 28-41.

(18) Huang, M.; Fong, C.; Khor, E.; Lim, L. Transfection efficiency of chitosan vectors: Effect of polymer molecular weight and degree of deacetylation. *J. Controlled Release* **2005**, *106*, 391-406.

(19) Rudzinski, W. E.; Aminabhavi, T. M. Chitosan as a carrier for targeted delivery of small interfering RNA. *Int. J. Pharm.* **2010**, *399*, 1-11.

(20) Liu, X.; Howard, K. A.; Dong, M.; Andersen, M. Ø.; Rahbek, U. L.; Johnsen, M. G.; Hansen, O. C.; Besenbacher, F.; Kjems, J. The influence of polymeric properties on chitosan/siRNA nanoparticle formulation and gene silencing. *Biomaterials* **2007**, *28*, 1280-1288.

(21) Jiang, X.; Dai, H.; Leong, K. W.; Goh, S.; Mao, H.; Yang, Y. Chitosan-g-PEG/DNA complexes deliver gene to the rat liver via intrabiliary and intraportal infusions. *J. Gene Med.* **2006**, *8*, 477-487.

(22) Berthold, A.; Cremer, K.; Kreuter, J. Preparation and characterization of chitosan microspheres as drug carrier for prednisolone sodium phosphate as model for anti-inflammatory drugs. *J. Controlled Release* **1996**, *39*, 17-25.

(23) Katas, H.; Alpar, H. O. Development and characterisation of chitosan nanoparticles for siRNA delivery. *J. Controlled Release* **2006**, *115*, 216-225.

(24) Bozzola, J. J.; Russell, L. D. Electron Microscopy : Principles and Techniques for Biologists.

(25) Dalby, B.; Cates, S.; Harris, A.; Ohki, E. C.; Tilkins, M. L.; Price, P. J.; Ciccarone, V. C. Advanced transfection with Lipofectamine 2000 reagent: primary neurons, siRNA, and high-throughput applications. *Methods* **2004**, *33*, 95-103.

VITA

Adriana Soliz was born on Memorial Day, May 27, 1985 in Corpus Christi, TX. She is the daughter of Juan Gilberto 'Gilbert' Soliz and Raquel 'Rachel' Ramirez Soliz. Before graduating high school, Adriana completed dual credit courses at Coastal Bend College in Alice, TX in the summer of 2001 and fall 2002. Adriana graduated from Alice High School in May 2003 and subsequently began her undergraduate work at Baylor University in Waco, TX in the fall. She also attended Del Mar College in Corpus Christi, TX during the summers of 2004 and 2005. In May 2008, Adriana received a Bachelor of Arts degree in Biology with a minor in chemistry. During the next two years, she worked as pharmacy technician with Scott & White Healthcare in Temple, TX and with Moore's Pharmacy in Sinton, TX. Also during that time she took some post baccalaureate classes at Baylor University (spring 2009) and at Texas A&M University Kingsville (summer 2009). Adriana entered the Graduate College at Texas State University-San Marcos in August 2010. In September 2010, she married her college sweetheart (Aaron R. Palacios, BSECE) and changed her name to Adriana Soliz Palacios.

Permanent E-mail Address: Adriana_17_2003@yahoo.com

This thesis was typed by Adriana Soliz Palacios.